DESIGN OF MINIATURIZED SWEEPING LANGMUIR PROBE AND ELECTRIC

FIELD PROBE FOR THE SPORT MISSION

by

Nathan P. Tipton

A thesis submitted in partial fulfillment
of the requirements for the degree

of

MASTER OF SCIENCE

in

Electrical Engineering

Approved:

_____   _____
Charles M. Swenson, Ph.D.   Ryan Davidson, Ph.D.
Major Professor   Committee Member

_____   _____
Jonathan Phillips, Ph.D.   D. Richard Cutler, Ph.D.
Committee Member   Interim Vice Provost for Graduate Studies

UTAH STATE UNIVERSITY
Logan, Utah

2021

ABSTRACT

Design of Miniaturized Sweeping Langmuir Probe and Electric Field Probe for the

SPORT Mission

by

Nathan P. Tipton, Master of Science

Utah State University, 2021

Major Professor: Charles M. Swenson, Ph.D.
Department: Electrical and Computer Engineering

The Scintillation Prediction Observation Research Task (SPORT) is a joint United States of America and Brazil 6U CubeSat mission. The US is providing the science instruments and the spacecraft launch. Brazil is providing the spacecraft bus, integration, and operations. Utah State University will provide four instruments for the mission as part of the US contribution in a suite called the Space Weather Probes (SWP). These instruments are the Sweeping Langmuir Probe (SLP), the Electric Field Probe (EFP), and the Sweeping Impedance Probe (SIP). Higher frequency components of the SLP and EFP will be observed through a Wave Spectrometer (WS). These instruments will provide measurements of electric fields, temperature, and density of ionospheric plasma. This thesis will describe the design, implementation, testing and calibration of the SLP, EFPs, and WS for the SPORT mission. A summary of results is also presented to show fulfillment of mission and instrumentation requirements.

(100 pages)

PUBLIC ABSTRACT

Design of Miniaturized Sweeping Langmuir Probe and Electric Field Probe for the
SPORT Mission

Nathan P. Tipton

The Scintillation Prediction Observation Research Task (SPORT) is a joint United States of America and Brazil 6U CubeSat mission. The US is providing the science instruments and the spacecraft launch. Brazil is providing the spacecraft bus, integration, and operations. Utah State University will provide four instruments for the mission as part of the US contribution in a suite called the Space Weather Probes (SWP). These instruments are the Sweeping Langmuir Probe (SLP), the Electric Field Probe (EFP), and the Sweeping Impedance Probe (SIP). Higher frequency components of the SLP and EFP will be observed through a Wave Spectrometer (WS). These instruments will provide measurements of electric fields, temperature, and density of ionospheric plasma. This thesis will describe the design, implementation, testing and calibration of the SLP, EFPs, and WS for the SPORT mission. A summary of results is also presented to show fulfillment of mission and instrumentation requirements.

To my wife, Allie. None of this would have been possible without her support and sacrifice.

ACKNOWLEDGMENTS

Many people have helped me get to this point and deserve recognition. Dr. Charles Swenson for giving taking a chance on me, giving me an opportunity to find my passion and mentoring me along the way. Dr. Jonathan Phillips, for the many hours of helping me figure out why nothing is working correctly. Caleb Young, for working along side me from the beginning, it would have been impossible without his help. My grandpa, for encouraging me to develop my curiosity and providing "inventors kits". My parents, for supporting my dreams every step of the way and letting me take everything apart as a kid. My wife, for her patience during all the long nights and supporting me while I pursue my passion.

Nathan P. Tipton

CONTENTS

LIST OF TABLES

LIST OF FIGURES

ACRONYMS

ADC	Analog to Digital Converter
ASSP	Auroral Spatial Structures Probe
DAC	Digital to Analog Converter
DICE	Dynamic Ionosphere CubeSat Experiment
EFP	Electric Field Probe
FIFO	First In, First Out data structure
FPP	Floating Potential Probe
FPGA	Field Programmable Gate Array
NTE	Not to Exceed
SIP	Sweeping Impedance Probe
SDL/USU	Space Dynamics Lab / Utah State University
SLP	Sweeping Langmuir Probe
SOC	System-on-chip
SPORT	Scintillation Prediction Observation Research Task
SWP	Space Weather Probes
WS	Wave Spectrometer

CHAPTER 1

INTRODUCTION

The ionosphere is part of Earth's upper atmosphere existing between approximately 80 and 1000 km in altitude. It is the Earth side of the edge of space where satellites orbit. The ionosphere is defined by the freely moving ions and electrons in what is called a plasma, a state of matter consisting of both charged and neutral atoms of a gas. These ionized atoms are created by a process called photoionization that occurs when high energy photons from the sun, X-rays, UV, and shorter wavelengths dislodge electrons from neutral gas atoms of the Earth's upper atmosphere. This creates a positively charged ion from the atom and frees a negatively charged electron. The total number of electrons and ions in the ionosphere are approximately equal given that they are originally both components of a neutral atom and the ions are singly ionized. The physics of the ionospheric plasma is complex because it is a charged gas that interacts with both electric and magnetic fields while its motions and density variations can create these fields. The weather of the ionosphere, defined by winds, temperature, and density changes within it, changes daily. The ionosphere's weather is driven by both the terrestrial weather below and by the solar wind coming from the Sun. The study of these processes is called Space Weather and involves complex computer models and a variety of observations of the ionosphere including ground-based radars and satellites carrying dedicated space weather instrumentation. The radio communications from satellites must pass through the Earth's ionosphere to reach radio antennas on the surface of the earth. Radio waves interact with the freely moving electrons in the ionosphere through the oscillating electric field of the electromagnetic wave. If the radio waves are of high enough frequency, then the inertia of the electrons does not let them interact with the radio waves allowing them to pass through the ionosphere unaffected. Lower frequency waves interact strongly with the electrons and will be refracted, reflected, or absorbed depending on the frequency of the waves and the conditions of the ionosphere. Satellites

generally use 100 MHz or greater frequency radio waves for communications which typically only experience some minor refractive bending of their ray paths. However, there is an extreme space weather event that happens near the equator of the Earth at night that affects even high frequency communications. Bubbles of low-density plasma originating at the bottom of the ionosphere rise in plumes that are tens of kilometers across and hundreds of kilometers high over the period of a few hours. These structures interfere with the radio waves causing rapid variations in signal power called scintillations. The process of scintillation is similar to light passing through water. When water is still and calm, it is transparent to light but when it is disturbed with bubbles, it is no longer transparent and the ability to see through the water is hindered even though both air and water are transparent to light. Severe scintillation conditions can prevent a GPS receiver from locking on to the signal and can make it impossible to calculate a position. Less severe scintillation conditions can reduce the accuracy and the confidence of positioning results. Plasma bubbles impact low-latitude countries, such as Brazil, by disrupting everyday navigation or limit potential GPS use in precision farming and self-driving vehicles. The triggering mechanism for plasma bubbles is of great scientific interest given that bubbles do not happen every night or at every longitude around the Earth.

1.1 SPORT Mission

The Scintillation Prediction Observation Research Task (SPORT) is a joint 6U CubeSat mission between the United States of America (USA) and Brazil. The science goals of this space weather mission are to investigate the conditions that lead to the formation of plasma bubbles.The scientific instrumentation si being developed by organizations in the USA: Utah State University (USU), University of Texas - Dallas (UTD), Goddard Space Flight Center (GSFC). In Brazil, the organizations are Instituto Tecnológico de Aeronáutica (ITA) and Instituto Nacional de Pesquisas Espaciais (INPE), who will provide the spacecraft, flight computer, and ground station. The SPORT program was selected by NASA HQ in December of 2016. USA partners received funding in the fall of 2017. Funding for Brazil was received in early 2018. The required U.S.A.-Brazil Framework Agreement allowing the

two countries to work together was ratified in April 2018 and was signed in early in 2019. Delivery of the completed USA instruments to Brazil is expected in early June and July 2020 with a possibility of earlier integration for the instruments being provided by USU. Delivery of the spacecraft for launch is expected to occur by December 2020, with launch occurring in the last quarter of 2021.

1.1.1 SPORT Science Overview

The SPORT mission has two specific questions it is trying to answer to understand the preconditions leading to equatorial plasma bubbles and scintillation.

1. What is the state of the ionosphere that gives rise to the growth of plasma bubbles that extend into and above the F-peak at different longitudes?

2. How are plasma irregularities at satellite altitudes related to the radio scintillations observed passing through these regions?

Answers to these questions will improve the ability to predict the formation of plasma bubbles and understand the conditions which develop anomalies in the ionosphere at low latitudes near the equator and lead to scintillations of radio signals.

The SPORT satellite will be used to address the first science question by making measurements of the state of the ionosphere when the satellite is in the region where plasma bubbles are thought to be triggered. On the next satellite orbit, the Earth's rotation moves that longitude sector to east and later into the night where fully formed bubbles might be present. A GPS receiver will be used to detect if bubbles have occurred by looking for scintillations on GPS signals coming from that direction. The data from many periods will be compared to look for patterns of why bubbles occur or do not occur at different longitudes around the Earth's equator. The second science question will be addressed by using measurements of the plasma density at the SPORT satellite produced at higher sample rates that have previously been obtained. This will permit the characterization of turbulence created by plasma bubbles with scale sizes down to 200 m. Radio receivers on the ground in Brazil will record the scintillation pattern on waves that pass through

the ionosphere and these will be compared to the satellite measurement of the turbulent plasma. Once verified using available data in the Brazilian sector, the same procedures can be applied at other longitudes to produce a global description of scintillation due to plasma bubbles.

1.1.2 Science Measurement Objectives

The SPORT mission is carefully laid out with instruments selected to provide the measurements needed for the science mission. Table 1.1 provides a compact form of the science questions and relation to the measurement requirements of the SPORT spacecraft instrumentation. These requirements are used to develop measurement requirements for each of the individual payloads of the satellite.

Table 1.1: SPORT Science Measurement Objectives

The Scintillation Prediction Observation Research Task (SPORT)		Instrumentation	Spacecraft
Observational Approach	**Science Measurement Requirements**	**Instrument Approach**	**Space Systems Requirements**
1) What is the state of the ionosphere that gives rise to the growth of plasma irregularities that extend into and above the F-peak?			
Observations in the 1700 to 0100 LT sector over -30° to 30° latitude Height profiles of the plasma density to specify the magnitude and height of the F peak density in the EA Vertical ion drifts at or below the F peak in the EA	**Plasma Density Profile** 1) 140 to 450 km alt 2) 10^4 to 10^7 p/cm^3 range 3) 20% p/cm^3 accuracy 4) 1000 km along track sampling **Ion Drifts (Earth Reference Frame)** 1) ±800 m/s Range 2) 20 m/s precision & accuracy 3) 10 km along track sampling	**GPS Occultation** Observe GPS satellite occultation along and to the sides of the orbit plane to obtain line of site TEC **Ion Velocity Meter** Observe vertical ion drifts by angle of arrival of heavy ions at detector	**Satellite Orbit** 1) ≥1 year mission life 2) 40° to 55° inclination 3) 350 to 450 km altitude 4) ±10 km eccentricity **Spacecraft** 1) ±5~~15~~° Ram Pointing 1σ 2) ≤1 km position knowledge 3) ≤10 ms timing
2) How are plasma irregularities at satellite altitudes related to the radio scintillations observed passing through these regions?			
Observations in the 2200 to 0200 LT sector over -30° to 30° latitude Observations of irregularities in electron density and E-field power spectral density in slope from 200 km to 200 m	**E-Field (Earth Reference Frame)** 1) ±45 mV/m range 2) 1.1 mV/m precision & accuracy 3) 1 km along track sampling 4) 10 km - 200 m along track waves **Plasma Density** 1) 10^3 to 10^7 p/cm^3 range 2) 10^3 p/cm^3 precision & accuracy 3) 1 km along track sampling 4) 10 km - 200 m along track waves **B-field** 1) ± 56,000 nT range 2) ±100 nT precision and accuracy 3) 1 km along track sampling	**E-Field Double Probe** Observe probe floating potential for AC E-fields from irregularity **GPS Occultation** S4 scintillation index **Langmuir/Impedance** Observe DC and AC probe response for relative and absolute electron density and observe irregularities **Three Axis Magnetometer** Support VxB computation for ion velocity and E-Field measurements	**Spacecraft Mechanisms** 1) ≥0.6 m tip-to-tip booms **Attitude** **(Post Flight Knowledge)** 1) ≤ 0.05° 1σ-uncertainty

The instruments on the SPORT spacecraft are: the Ion Velocity Meter (IVM), the Compact Total Electron Content Sensor (CTECS), the Electric Field Probe (EFP), the Sweeping Langmuir Probe (SLP), the Sweeping Impedance Probe (SIP), and the Magnetic

Field probe(Fluxgate).

The Ion Velocity Meter is provided by the University of Texas at Dallas (UTD). The instrument measures the motion of the ions, or winds, within the ionospheric plasma. The Compact Total Electron Content Sensor (CTECS) is provided by the Aerospace Corporation. CTECS is a GPS receiver that is used to detect both scintillation and obtain electron density profiles using radio occultation techniques. Goddard Space Flight Center is providing the Magnetic Field probe. This instrument will measure the ambient magnetic field using a fluxgate magnetometer deployed on the SLP boom. Utah State University is providing the EFP, SLP, and SIP. The SIP measures the absolute electron density local to the spacecraft. The SLP measures relative plasma density, temperature, the floating potential, and space potential. The EFP measures one component of the vector DC and AC electric fields.

Figure 1.1 shows the location of all the science payloads on the SPORT spacecraft and the organization responsible for the instrumentation development.
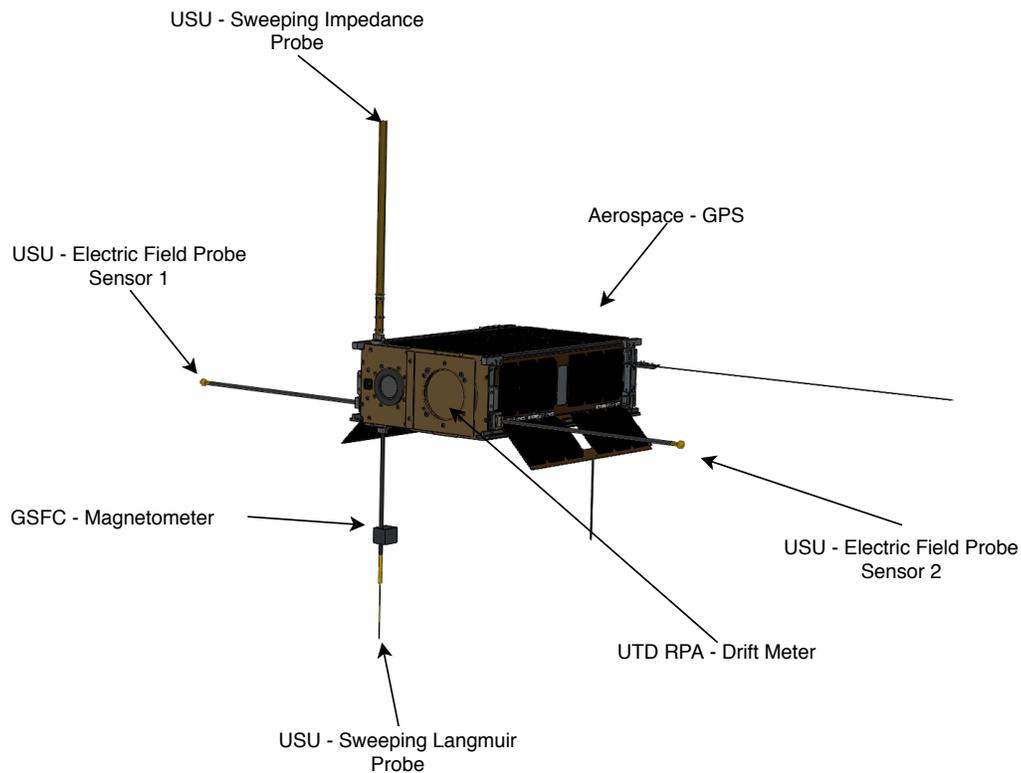
Fig. 1.1: SPORT Spacecraft and instruments

1.1.3 The USU Space Weather Probes

The Space Weather Probes(SWP) is the name of the collection of instruments and measurements provided by USU. The SWP is composed of the Sweeping Langmuir Probe that produces both DC current measurements in the electron saturation region and IV curves from a voltage sweep. The Electric Field Probe provides a monitor of the floating potential of the spacecraft during the voltage sweep of the Langmuir Probe and provides a measurement of the electric field along one axis. The wave Spectrometer is an on-board computation of both the high frequency electron density and electric field wave spectrum. The Sweeping Impedance Probe provides observations of fundamental plasma resonances that occur at RF frequencies. Table 1.2 provides a summary of the science requirements for the USU SWP. These requirements are a flow down from the SPORT Science Measurement Requirements of Table 1.1.

Table 1.2: SPORT science requirements and objectives for Electric Field Probe and Sweeping Langmuir Probe

Parameter	EFP	SLP	SIP
Scientific Measurement Requirements	**Electric Fields** 1. ±45 mV/m range 2. 1.1 mV/m precision **Waves** 1. 10 km - 200 m sampling	**Plasma Density** 1. 10^3 to 10^7 p/cm^3 range 2. 10^3 p/cm^3 precision 3. 1 km sampling **Waves** 1. 10 km - 200 m sampling	**Plasma Density** 1. 10^3 to 10^7 p/cm^3 range 2. 10^3 p/cm^3 precision 3. 200 km sampling
Measurement Objectives	0.1 to 500 mVm, 1% V_i (derived): 20 m/s	ΔN_e :10 to $10^7 cm^{-3}$, 5% ΔN_i : 10^3 to $10^9 cm^{-3}$,5% T_e : 200 to 5000 K V_f : ±10 mV to ±12 V V_n : ±10 mV to ±12 V	N_i : 10^3 to $10^9 cm^{-3}$,5% 1 km sampling
	DC - 40 Hz	DC - 40 Hz, 25 s/sweep	DC - 40 Hz, 25 s/sweep
	16 spectral bins 20 Hz to 15 kHz	16 spectral bins 20 Hz to 15 kHz	

The SPORT mission is being implemented using a 6U spacecraft that has limited mass, power, and telemetry resources. A conceptual design of the SPORT mission was contained in the original proposal to NASA including an allocation of resources for the USU space weather probes. The power allocation was 0.7 W orbit average with an on-orbit telemetry collection allocation of 3502 bits/s while the mass allocation from the proposal was 320 grams. An interface control document was developed as part of the detailed design process of the space weather probes. New allocations were developed as the probe designs matured for the utilization of resources. The mass resources are presented in Table 1.3 and describe the low-mass probes and hinges as well as the mass of the electronics board. The not to exceed mass was 234 grams and the measured values of the components came in 8% less than the value allocated. Mass has not been a critical resource for the SPORT mission. The spacecraft telemetry resources were not considered a critically tight resource for SPORT. The proposed X-band downlink data rate and ground stations provided more than 100%

margin at the conceptual design stage. The not to exceed allocation for the space weather probes was 40 kbits/s of continuous telemetry while the proposed utilization was 26.5 kbit-s/s. These allocations are presented in Table 1.5 and show that the margin on the telemetry allocation was 34%.

Power has generally been the most critical resource for the SPORT mission and also for the Space weather probes. The probe was designed to run from an unregulated voltage source in the range of 12 to 16.8 and the not to exceed allocation for the probe was a current draw of 140 mA. This gave a power consumption of 1.68 W orbit average power or more than twice the conceptual design value. What was more surprising was that the actual current draw exceeded this amount by 11% as shown in Table 1.4. The reason for this over budget on power has not been definitively determined but appears to be related to the current draw of the analog section of the Langmuir probe.

Table 1.3: USU SWP Mass Allocation

Mass		
Experiment Component	Quantity	Current Mass Per Unit (g)
Main PCBA with Daughterboard	1	57
SLP Boom without Hinge	1	31.8
EFP Boom without Hinge	2	12
SIP Boom without Hinge	1	46.5
Boom Hinges	4	14
Total Mass (g)		**215.3**
Total Mass NTE (g)		**234**
Total Margin		**8%**

Table 1.4: USU SWP Power Allocation

Power			
Voltage Supply	Current (mA)	NTE (mA)	Margin
Unregulated @ 12V	155	140	-11%
Unregulated @ 16.8 V	118	106	-11%
5V	0.0025	0.005	50%
3.3V	3.8	8	53%

Table 1.5: USU SWP Telemetry Rate Allocation

Telemetry Rate			
Interface	Current (bps)	NTE (bps)	Margin
SPI to spacecraft	26483	40000	34%

1.2 Instrument History and Literature Review

The USU SWP is both the miniaturization and the collection of multiple science instruments onto a single electronic circuit board. Historically these have been separate instrumentation packages when flown on spacecraft but with the development of miniature spacecraft in the form of CubeSats there has been a need to similarly miniaturize the scientific probes for measuring the space environment. The designs of the SWP are an evolution of the designs and lessons learned from multiple past missions. We briefly review the most recent history contributing to the USU SWP development

1.2.1 Past Langmuir Probes

Langmuir probes have been used for many years as the primary method for in-situ measurement of the ionospheric plasma density and temperature. Langmuir probes have been flown on both sounding rockets and satellites by many organizations and the tech-

nique for measuring space plasma temperature and density has been reviewed by Brace. [1] Utah State University has a history of flying Langmuir probes together with Impedance probes on sounding rockets stretching back 60 years. The USU SWP draws from Langmuir probe designs which have recently been flown on both the Dynamic Ionosphere CubeSat Experiment (DICE) and the Auroral Spatial Structures Probe (ASSP).

Dynamic Ionosphere CubeSat Experiment (DICE)

DICE was a CubeSat mission to study the Earth's ionosphere developed by ASTRA and USU/SDL which was funded by the NSF and launched by NASA. The mission consisted of two identical 1.5U CubeSats launched into a high inclination low Earth orbit in 2011. Both spacecraft carried two spherical Langmuir probes deployed from each end of the 1.5U CubeSat to measure plasma densities from 1 x $10^4 cm^{-3}$ to 2 x $10^7 cm^{-3}$. The probes had a dynamic range of $\pm 50 uA$ and sensitivity of $1.525 nA$. The DICE Langmuir probes had a power budget of 40 mW. The probe sensors were 1.27cm gold plated aluminum spheres, positioned 13 cm away from top of spacecraft and 21 cm away from the center. [2–4]

Auroral Spatial Structures Probe (ASSP)

The Auroral Spatial Structures Probe was a NASA sounding rocket mission launched in 2015 to study the Earth's electric and magnetic fields during an Aurora. The mission was composed of a main payload and six cylindrical sub payloads that were approximately 6 inches in diameter and 5 inches tall. Each sub payload had a fixed bias Langmuir probe. The sensor was a 1-inch sphere positioned on a mast and aligned with the spin axis of the sub payload. The Main payload had multiple fixed bias Langmuir probes collecting from six different segments of a cylinder sensor. This configuration was called a fast temperature probe. A separate sweeping Langmuir probe was also included collecting from a cylindrical tip sensor. [5]

1.2.2   Past Electric Field Probes

The double-probe class of in-situ electric field instruments has been used for decades

to observe electric fields in the space environment (Fahleson 1967). It operates by making measurements of the potential difference between two isolated, separate conductive sensors immersed in the plasma that are electrically isolated from the spacecraft electronics. Electric Field double Probes have been also flown on DICE, ASSP and the STORMS sounding rocket.

Dynamic Ionosphere CubeSat Experiment (DICE)

Two boom sets of Electric field probes utilizing the Double probe technique were used on the DICE spacecraft. Probe measurements were filtered using an analog chain before being digitized and sent to the onboard FPGA. The probe had a power consumption limit of 40 mW and an area limit of $16cm^2$. The probes used gold plated spheres with a 1 cm diameter. The booms were wire booms the deployed to 5m from center of spacecraft and 10m tip to tip. [2, 3]

Auroral Spatial Structures Probe (ASSP)

Each of the six sub payloads and the main payload of ASSP carried a crossed set of Electric Field probes. The sub payload used wire booms and the main payload had a set of rigid folding booms.
The instrumentation and the wire boom system were derived from the DICE mission. [5] The electronics made use of the INA116 developed by Burr-Brown as an ultra low input bias current instrumentation amplifer as implemented for DICE.

STORMS

STORMS was a NASA sounding rocket mission to investigate mid-latitude ionospheric irregularities associated with terrestrial weather systems. The STORMS SDL/USU payload had 4 Floating Potential probes. The ambient electric field was found by taking the difference between the probes in post processing due to a higher number of electric field probes. [6]

1.2.3 Past Plasma Wave Spectrometers

Plasma Wave Spectrometers do not have a history of being flown on CubeSats due to implementation complexity and power limitations but have been flown on larger satellites including Voyager 1, Cassini, and Wind.

Dynamic Ionosphere CubeSat Experiment (DICE

DICE had a spectrometer on the electric field channel. The instrument used a 1024-point FFT with 4 spectral bins and a frequency range of 16 Hz - 512 Hz. [2,3]

Voyager 1

The Voyager Plasma Wave System used a 16-channel spectrum analyzer with a frequency range of 10 Hz to 56 kHz. This plasma wave instrument alone used between 1.1-1.6 W of power. The instrument size was 31.8 cm x 18.5 cm x 4.8 cm with a mass of 1.4 kg. [7]

Cassini

Cassini improved on the wave spectrometer from the Voyager spacecraft. The Cassini plasma wave instrument had 16 logarithmic spaced channels with a range of 10 Hz to 56.2 kHz. The main electronics of this science payload were 5 kg, 41.7 cm x 17.8 cm x 16.8 cm, and had a peak power consumption of 5.09 W. [8]

WINDS

The WAVES investigation on the WIND spacecraft uses a 1024-point FFT receiver with a frequency range of DC- 10 kHz implemented with a DSP. The frequency spectrum is divided into three bands [9]

1.2.4 SPORT Improvements

SPORT will include a cylindrical Langmuir probe with both sweeping and fixed bias capability, a double spherical Electric Field probe, and a Wave Spectrometer with 16 spectral bins. The SPORT Space Weather Probes is drawing significantly from the designs

utilized on DICE and ASSP missions. Both DICE and ASSP integrated Langmuir, Electric field probes, and Magnetic field sensors onto a single circuit board. SPORT will include an impedance probe. Many of the changes and improvements will be implemented in the onboard FPGA system on module within the digital signal processing chains as well as instrument control, data packetization, and time stamping. The amount of filtering on the SLP and EFP will be increased to reduce noise with most of the filtering occurring in the FPGA fabric. Signals will be digitized earlier in the processing chain compared to previous designs. In addition to the added filtering, SPORT will have increased data rates for the SLP and EFP, thereby providing a more detailed picture of the plasma density and bubble structure. Another major change compared to previous iterations is the addition of a 16 channel wave spectrometer channel which will be an expanded and improved version of the DICE spectrometer, allowing for the feasibility of implementation of a Wave Spectrometer within the limitations of a CubeSat form factor to be explored. The SLP and EFP electronics, together with the SIP, magnetometer, and real time clock, will be combined on one 9 cm x 9 cm PCB. For information on the Sweeping Impedance Probe, see the thesis discussing the development of that instrument for SPORT.

1.3 Thesis Outline

This thesis is documentation of the process undergone during the development of the Sweeping Langmuir Probe, Electric Field Probe, and Plasma Wave Spectrometer. While focused on these instruments, additional information on the development of the USU Space Weather Probes as a whole is provided. Chapter 2 provides an overview of the system architecture, including power conditioning, mechanical design, and firmware, as well as the concepts of operation for testing and analysis of data products. Chapter 3 discusses the Sweeping Langmuir Probe, beginning with a brief overview of the concept of operation. The rest of the chapter discusses the analog and digital components of the instrument and all the design, decisions, and analysis involved. The chapter ends with the calibration of the probes including all methodology and results. The Electric Field Probe and Plasma Wave Spectrometer comprises Chapters 4 and 5, following the same outline as Chapter 3.

Chapter 6 contains a summary of the thesis concluding with final Space Weather Probes performance review, lessons learned, and future work.

CHAPTER 2

INSTRUMENT ARCHITECTURE AND CONCEPTS OF OPERATION

The Utah State University Space Weather Probes Instrument architecture and the concepts of operation are presented within this chapter. The high-level objectives for the SWP were to integrate the previous instrument developments of the DICE and the ASSP missions into a single printed circuit board that would be mechanically compatible with the CubeSat standard. The integrated instrument was to be a stand-alone module within a CubeSat with clean interfaces, its own instrument controller, and an isolated power supply. Given that the SWP is a suit of instruments, it was desired to have control over each of the individual components with the ability to power down and control the production of telemetry through software commands. Within this chapter, we overview the approaches to the SWP starting with a general review of the instrumentation architectures and then moving to the mechanical layout and the deployed components. The architecture of the operational modes is presented, followed by a discussion of the telemetry and telecommand details. The chapter ends with a detailed discussion of the firmware architecture followed by a brief discussion of the testing approaches and how the observations of plasma density, temperature, fields, and waves will be produced to meet the science requirements and objectives from Table 1.2.

2.1 Architecture of Hardware and Power Conditioning

An architecture diagram of the SWP printed circuit board is present in Figure 2.1. The concept for controlling the SWP is through the use of an FPGA with an embedded microcontroller. The FPGA fabric is used to provide the real time control of the instruments and time stamping of telemetry data while the microcontroller would be used to both format telemetry packets and to receive telecommands from the spacecraft computer. The analog components of the electric field probe, the sweeping Langmuir probe, and the sweeping

impedance probe are shown on the left in Figure 2.5. These probes interface with the FPGA
via SPI for controlling both their digital to analog (DAC) and analog to digital converters
(ADC) within the instruments. Housekeeping temperature, voltage, and current monitors,
shown at the top in Figure 2.5 pass data to the FPGA controller. The collected telemetry
data is passed to the host spacecraft systems via an SPI protocol interface. Telecommand
from the host spacecraft are also received via the same SPI interface. The programing of the
FPGA and micro controller is through a USB interface and an onboard FTDI programmer
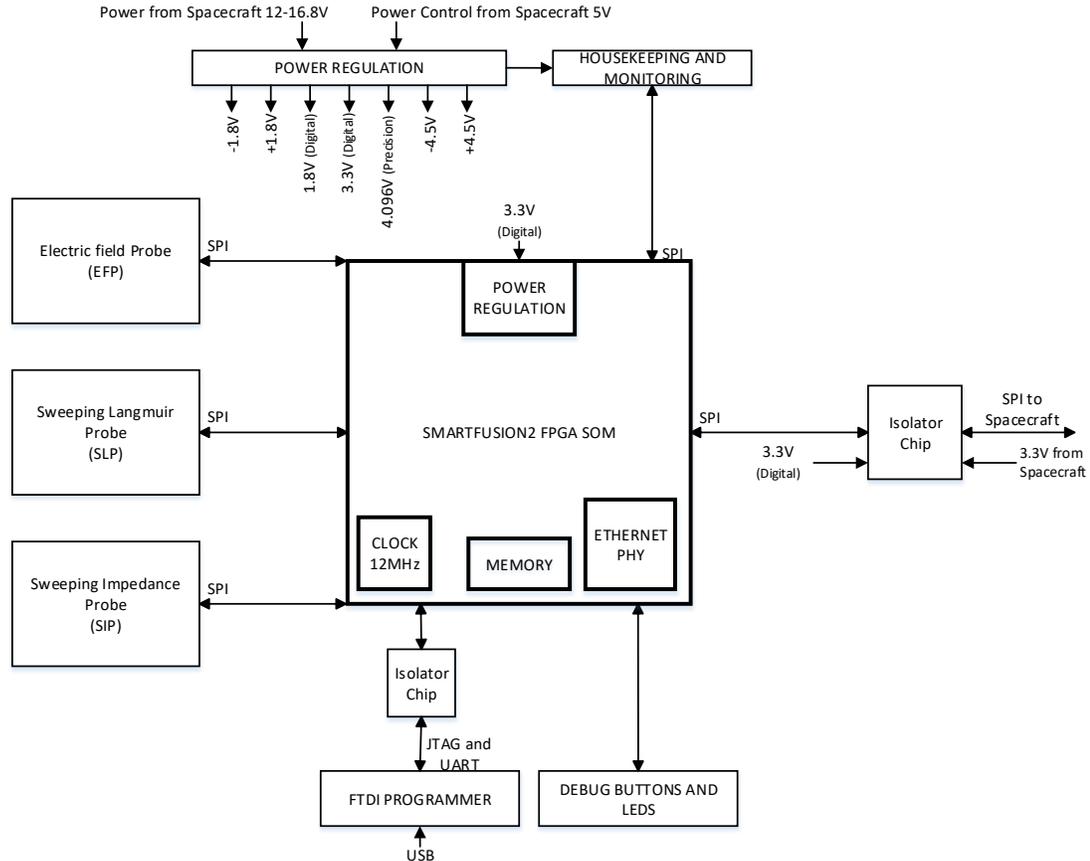system that is powered from the USB interface.

Fig. 2.1: Space Weather Instruments hardware architecture

2.1.1 Instrument Controller FPGA

A Smartfusion2 system-on-chip (SoC) composed of a flash-based FPGA and an ARM Cortex-M3 processor was selected based on both its low-power and the heritage of Microsemi's flash-based FPGAs use in space systems. A System-On-Module (SOM) from EmCraft was chosen which contains the SmartFusion2 SoC (FGG484 package), 64 MB of low power DDR memory, 16 MB of flash memory and a 10/100 Ethernet chip. The SOM is a small (30 mm x 57 mm) mezzanine module that can be either attached to the underside of the SWP PCB or to development board. This approach of using a SOM was chosen to both speed software and hardware development. The SOM provides all the power regulation necessary for operation of the SmartFusion 2 and it's supporting electronics when provided with 3.3 volts. The SOM interfaces with the SWP PCB instruments through two 80 pin inter-board connectors. The overall architecture of the USU SWP hardware is shown in Figure 2.1.

2.1.2 Instrument Electrical and Power Interface

The science instruments of the SWP make very low-level current and voltage measurements of the plasma in which the spacecraft is immersed in order to meet the scientific objectives. The measurements are made from deployed probe surfaces with return currents collected on the spacecraft structures. Therefore, it was decided to completely electrically isolate the SWP from the spacecraft's power and communication systems to avoid any noise that could introduced by ground loops or other spacecraft subsystems. Internally to the instrument, care was taken to separate analog power and grounds from digital power and grounds, as well as components on the PCB. Figure 2.2 presents the architecture of the electrical and power interfaces for the SWP as well as the internal voltages and power grounding schemes.

The USU SWP have been designed to be powered from an unregulated power bus of the spacecraft, with an input range of 12 - 16.8V, although the SPORT spacecraft is providing a regulated 12V input to the SWP. Two isolated DC-DC converters are used to create internal analog 5V and digital 3.3V power supply rails. The DC-DC converters are controlled with a

5V enable line from the spacecraft. The internal analog 5V rail is converted into a precision reference of 4.096 volts and regulated to produce positive and negative power supplies of $\pm 1.8V$ and $\pm 4.5V$. Dual output linear regulators provide these voltages to lower noise from the previous voltage regulation stages.

The 3.3V digital voltage is further down converted to 1.8V and used to power the digital components of the SWP including the SOM, DACs and ADCs.

The digital communication lines between the SPORT spacecraft and USU SWP are passed through a digital isolator chip to further isolate the spacecraft grounds from the instrument grounds. The spacecraft uses 3.3V to power its side of the chip while the SWP powers the internal side of the isolation chip. Within the USU SWP, a star grounding scheme was implemented to reduce noise in an attempt to reduce the noise in the sensitive analog sections. Analog and digital signals were physically kept separate on the circuit card to reduce EMI. The grounds for the analog and digital components are brought together only at one single point where they are also connected with the spacecraft electronics and spacecraft chassis ground. This star ground point can be seen in Figure 2.2 along with the power conditioning circuitry for the USU SWP.
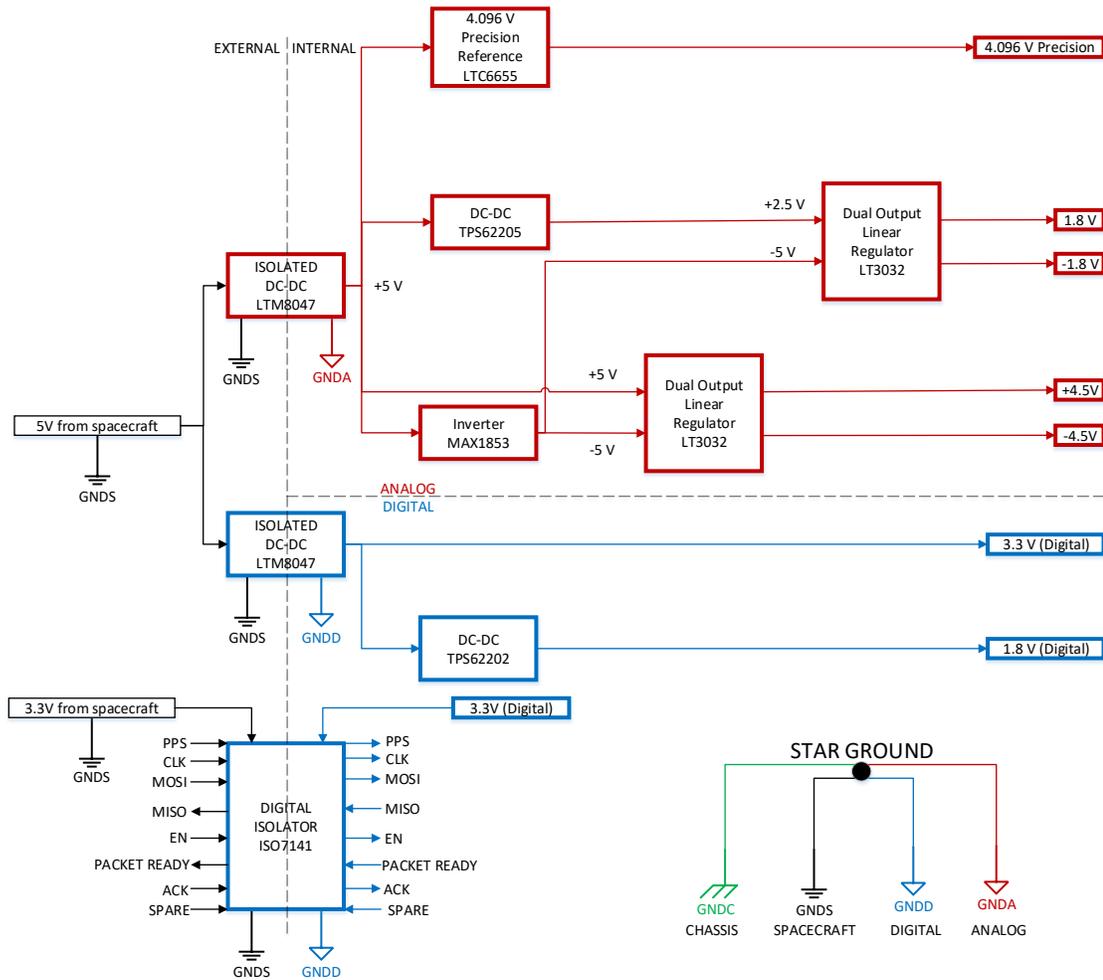
Fig. 2.2: Power Conditioning Architecture

2.2 Mechanical Architecture

The SWP consists of four sensors that fold out from its host spacecraft using miniature hinges together with a single printed circuit board as shown in Figure 2.3. The printed circuit board follows the PC/104 form factor standard (90 x 96 mm) for dimensions and mounting holes but does not include the electrical backplane connector called out by the standard. MMCX connectors are used to connect instruments to the external sensors probes which are located at the ends of the deployable booms.The mounting locations of the booms and sensor on the SPORT spacecraft are shown in Figure 1.1. The printed circuit board is

connected to the spacecraft systems using an Omnetics Nano-D connector which provides power and communication between the spacecraft and USU SWP. Its mate is provided to the spacecraft provider as a pigtail connector for integration into the spacecraft as shown in Figure 2.3.
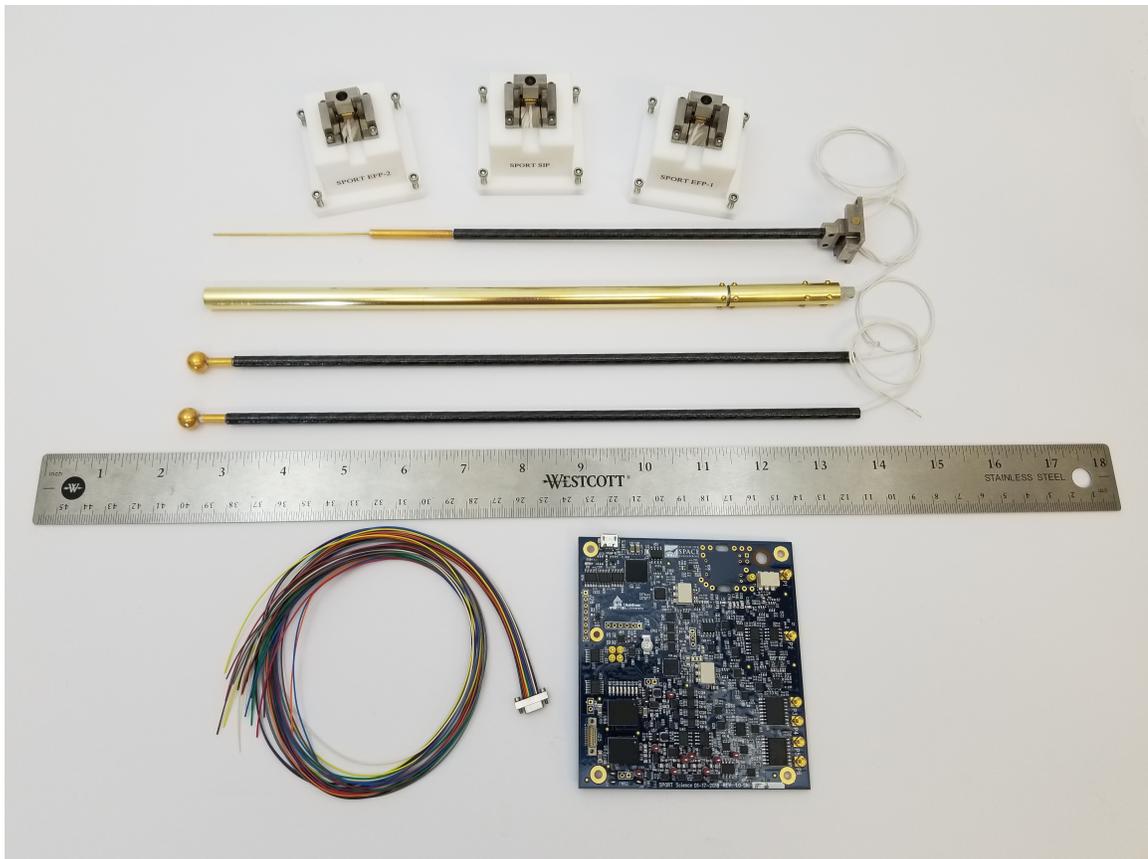

Fig. 2.3: USU SWP PCBA with Booms

Figure 2.4 details the various connectors placement on the SWP printed circuit board. Right angle MMCX connectors to coaxial cables are used for signals coming off of the board to conserve space and simplify cable routing. The Electric Field Probe consists of four connectors. The center conductors of EFP 1P and EFP 2P are electrically connected to the probe surfaces while the shields of the cables are driven guards used to reduce the capacitance of the cables. The connect to the gold-plated cylindrical shield sections just

below the gold-plated spherical sensors. The center conductors of EFP 1N and EFP 2N connect to the spacecraft structure while the shields are left isolated and unconnected. Similar to the EFP, the sweeping Langmuir probe (SLP) center conductor is connected to the gold-plated 76 mm long needle sensor at the end of the boom and the shield is a driven guard for the signal. It is connected to a gold-plated cylindrical shield section just below the needle probe as seen in Figure 2.3. The MMCX connections for the sweeping impedance probe are similar to the electric field probe in that the center conductor of the SIP A (A for antenna) is electrically connected to the 234 mm long impedance probe while the electrically driven shield is a guard which is attached the 50 mm long section at the base of the boom. The SIP G connector has the center conductor connected to the spacecraft chassis and the shield is left isolated and unconnected.

The spacecraft interface is through a single Nano-D connector and electrically through the mounting holes which electrically tie the board star ground to the spacecraft structural ground (see Figure 2.2). The ethernet header is unused while the micro USB programming port is to be routed to an external connector on the surface of the spacecraft for late reprogramming of the FPGA and processor as needed.
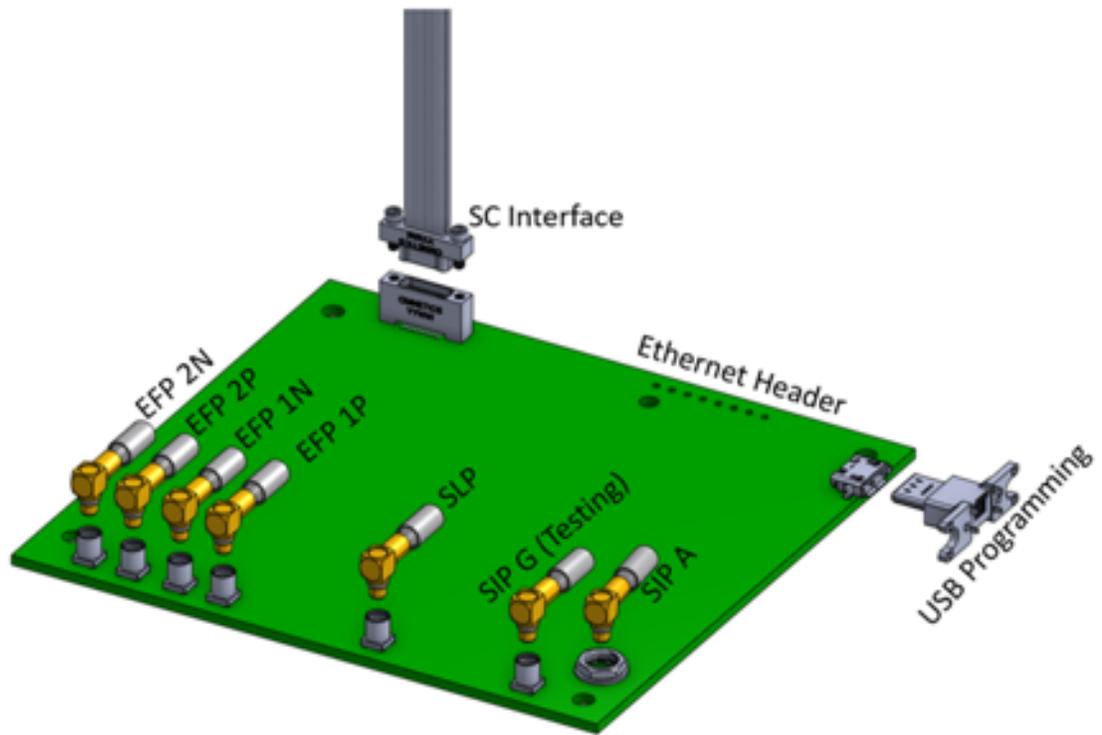
Fig. 2.4: USU SWP board with connectors

2.3 USU SWP Telemetry and Command Concept of Operations

The collection of instruments of the USU SWP produces a number of different types of data depending on the mode of operation or through onboard data processing. The approach taken was to use the Consultative Committee for Space Data Systems (CCSDS) recommended Space Packet Protocol to organize both the telemetry and the telecommand. The Space Packet Protocol (SPP) is designed as a self-delimited carrier of a data unit (i.e., a Space Packet) that contains an Application Process Identifier (APID) used to identify the data contents and data source. This a well-documented international standard uses a 6-byte header to identify the source of data as well as the length of the data packet. It is used to organized the data flowing from the instrument (telemetry) as well as the commands to the instrument (telecommand) that change operational modes and gains of the SWP.

2.3.1 Telemetry Concepts

The USU SWP produces 7 different types of SPP in order to meet the science requirements and objectives from Table 1.2, the USU SWP will produce the telemetry packets described in Table 2.1. Status packets provided general information about the SWP instrument including temperatures, current and voltage monitors, and perhaps most important: timing base synchronization information based on a one pulse per second signal from the spacecraft and an associated time message. The Science packets contain basic DC measurements at a 100 Hz rate from the Electric Field Probe, Sweeping Langmuir Probe,and the Magnetometer. The SLP Sweep packets consist of a set of Langmuir probe currents obtained during a voltage sweep along with associated floating potential measurements from the Electric Field Probe. The Wave packets contain spectrometer data using an on-board FFT analysis of both the Sweeping Langmuir Probe and the Electric Field Probe as the source. The SIP Sweep packets contain the measured in-phase and quadrature components of the current flowing to the probe over the frequencies defining the sweep. SIP Track packets contain a measurement of the frequency of the upper hybrid resonance as observed by the Sweeping Impedance Probe. The final packet type is the Config which reports the current gain and table data settings within the SWP which can be changed by telecommand from the ground.

Table 2.1: USU SWP telemetry packet contents,sizes, and rates

Packet Name	Packet Contents	Size (bytes)	Period (s)
Status	Housekeeping data: time synchronization, Operating modes, monitors and error flags	108	120
Science	SLP DC measurements Magnetometer XYZ and temp	1812	1
SLP Sweep	SLP Sweep measurements	10532	120
SIP Sweep	I and Q data	3084	120
SIP Track	Tracking Frequency	412	1
Wave	EFP and SLP Magnitude squared freq. bins	972	1
Config Echo	Current gain and Table data settings		NA

2.3.2 Telecommand Concepts

The USU SWP obtains commands in the form of SPP formatted packets to change the operational state of the instruments, reconfigure it, or to pass timing information. Only six type of packets are recognized as described in Table 2.1. Some packets are only to be used on the ground for calibration of the instrument while other packets can be used to upload new tables controlling the SLP voltage sweep and the SIP frequency sweep. The SWP operates in three different modes, Idle, Science, and Calibrate. The telecommands are used to switch between these modes. The modes of operation are shown in Figure 2.5 as a state machine with the telecommands being used to transition between the three states and to change configuration within states. Time GPS messages can be received in any state and are used to synchronize the clocks and time stamping systems internal to the SWP with GPS time during post processing of the telemetry.

Idle

The SWP enters the Idle state on power up. Upon entering the Idle state, a Status packet is generated to indicate a successful power up and provide initial housekeeping data. The current SWP configuration is also provided at power up in a generated Configuration

Table 2.2: Science Mode Measurements

Sweeping Langmuir Probe (SLP) Electric Field Probe (EFP)	
Measurement Technique	1. DC 2. Voltage Sweeps 3. Wave Spectrometer
Sweeping Impedance Probe (SIP)	
Measurement Technique	1. Frequency Sweeping 2. Resonance Tracking

Echo packet. The SWP after generating these two packets will wait in Idle state until a command to switch modes is received. From Idle, the SWP can either be put into Calibrate mode or Science Mode. The SWP must be in the Idle state before a new configuration can be applied.

Science

The SWP is normally expected to operate in the Science mode. This mode produces the telemetry packets previously described in Table 2.1 and is reached by sending a Science mode command while in Idle. The desired telemetry packets to be produced are selected by the data bytes in the Science mode command packet. To change the telemetry to be produced, the SWP must first be put back to Idle and a new Science mode command sent with the desired packets. Status packets are automatically produced while the SWP are in Science mode.

Table 2.2 shows the measurements that can be controlled for each instrument. DC is an operation of the Langmuir probe at a fixed bias with the Electric Field Probe operated as two floating potential probes that are all simultaneously sampled. Voltage Sweeps is an operation of the Langmuir probe obtaining a current voltage characteristic over a range of voltage steps with the Electric Field probe operated as two floating potential probes simultaneously sampled at each voltage step of the sweep. Wave Spectrometer is an operation of the Electric Field Probe as a double probe along with the fixed bias Langmuir probe to produce high frequency power spectra.Frequency Sweeping is an operation of the impedance probe over a range of frequency steps ordered into a sweep. Resonance tracking

is the operation of the Sweeping Impedance Probe in a closed loop tracking of the occurrence frequency of the upper hybrid plasma resonance. The current configuration can be read while in Science mode without switching back to Idle.

Calibrate

Calibrate mode is not used in flight. This mode is used for checkout, testing and calibration of the instrumentation during development. Individual parameters configurable through the uploading of a Configuration packet are also able to be configured individually while in Calibrate mode. Calibrate mode also provides the ability to manually step through sweeps of the SLP or SIP. Calibrate mode can only be set from the Idle state.
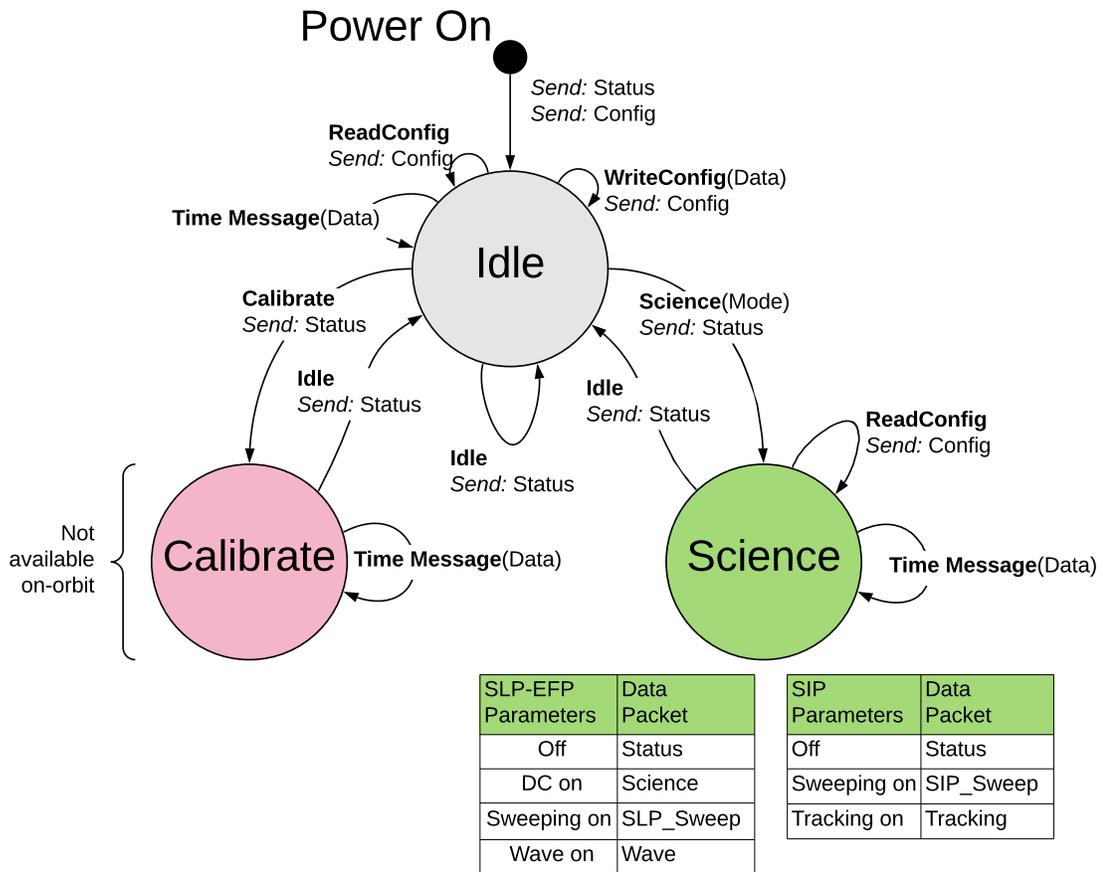

Fig. 2.5: USU SWP Modes of Operation

2.4   Firmware Architecture

The firmware consists of both the C-code and the FPGA HDL placed on the Smartfusion2 with its embedded ARM Cortex M-3 processor. This ARM processor controls all the communication with the SPORT spacecraft. It also formats the CCSDS Space Protocol Packets for telemetry and interprets the telecommand packets. Data is passed back and forth between the processor and the FPGA fabric via an internal data bus to the Smartfusion2. The processor runs in a single software loop entering a low power idle state at the end of the loop. When a hardware interrupt is generated, either by the FPGA fabric or by communications initiated by the spacecraft, the processor is woken and execution resumes. Conceptually the FPGA fabric operates the instruments and collects data, placing into a FIFO, one per instrument, in what is called a data granule. The fabric then generates an interrupt for the processor to indicate that a data granule is ready to be collected. A packet consists of many granules of data which the processor collects over time and formats to create a complete packet.

On power up of the SWP, the processor runs through initialization. This stage configures all the interrupts, GPIO pins, and FPGA instrument configuration parameters. After initialization, the processor proceeds with normal operation in the main loop.
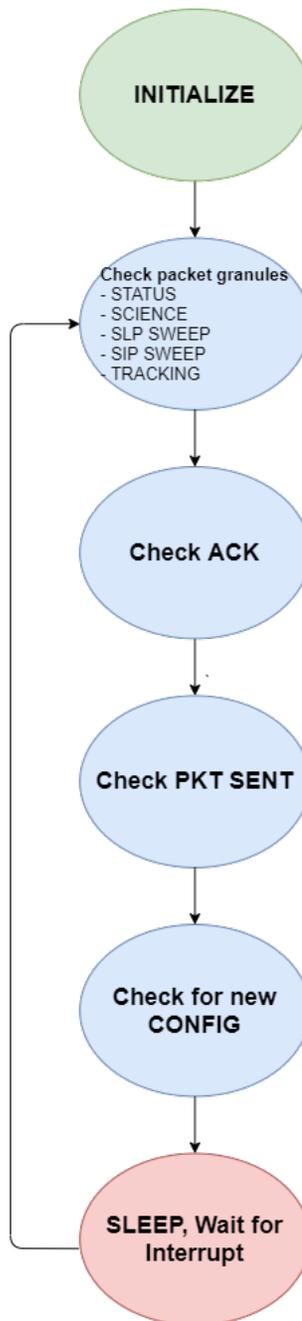
Fig. 2.6: Main processor loop

The main loop, as illustrated in Figure 2.6 checks for any packets complete and ready to be formatted with a SPP header and placed into an outgoing telemetry buffer. After checking each of the different packet statuses, the processor enters a sleep mode. The

processor remains in sleep mode until an interrupt is triggered. After handling the interrupt, the processor will run through all the checks before entering sleep mode again. This interrupt driven architecture is used to reduce power consumption in the processor by allowing it to remain in the sleep mode until needed.
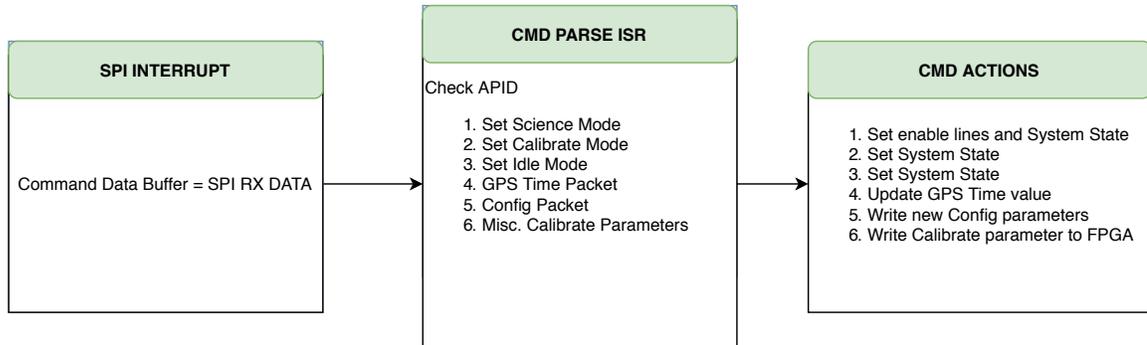

Fig. 2.7: Processor Commands

The SPORT spacecraft acts as the Master with the USU SWP as the Slave in the SPI communication. The SWP utilizes an interrupt to determine when the SPORT spacecraft has sent a command. After checking the checksum on the received command, the APID is checked. The APID determines the actions taken, whether calling a function, setting a register, or setting the level of a GPIO pin to the FPGA fabric.
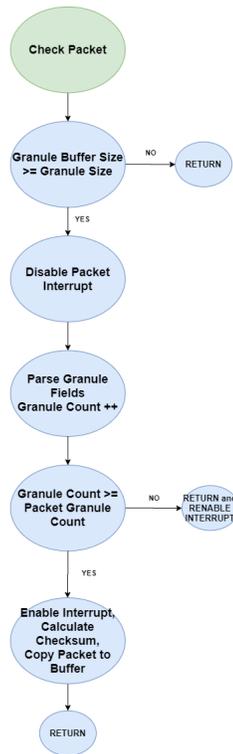
Fig. 2.8: Function to process granules/packets from granule buffer

The microprocessor and FPGA interface using FIFOs. Each packet type has its own FIFO. A whole packet is made of many smaller granules. The FPGA writes a granule, a 32-bit word at a time, into the FIFO. When the FIFO is not empty, the FIFO triggers an interrupt in the microprocessor. The ISR for each FIFO reads out the words from the FIFO into a granule buffer. In the main loop, a function is called to check each packet's granule buffer to determine if a whole granule has been read from the FIFO. The generic flow of this function is shown in figure X. If the buffer does not contain an entire granule, the processor returns to the main loop and checks the size of the buffer again on the next iteration. Once the size of the buffer is greater than or equal to a granule, the processor parses the buffer, putting the granule into the current packet being formed. Once the last granule in a packet has been received, the processor copies the packet into a packet buffer.
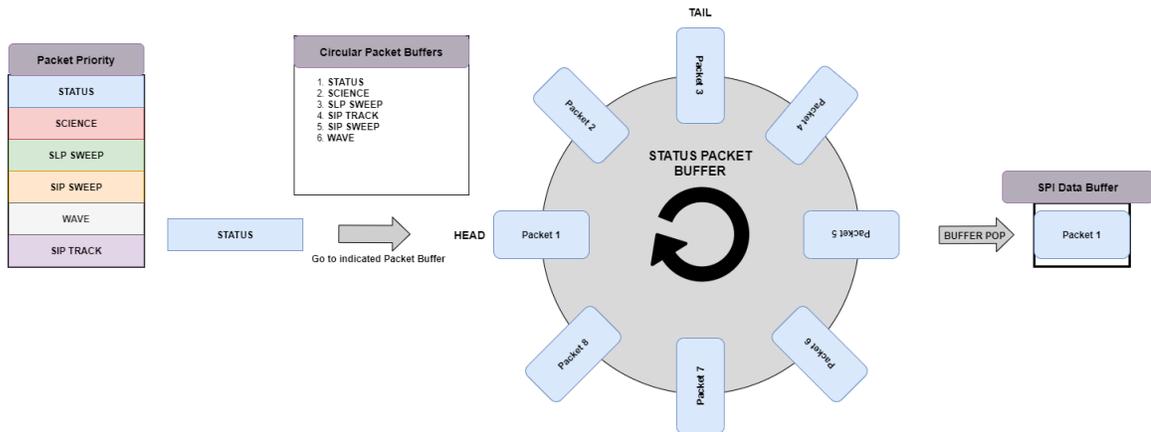
Fig. 2.9: Circular buffer for telemetry packets

To prevent data loss due to the SPORT spacecraft not reading from the USU SWP, a packet buffer stores finished telemetry packets. The buffer architecture is shown in figure 2.9. This packet buffer is a collection of circular buffers, one for each packet type. When a telemetry packet is created, a packet type counter is incremented. packet type counter keeps track of number of each type of packet in the buffer. The telemetry packet is then pushed onto the corresponding circular buffer. When a packet is ready to be sent to the spacecraft, the packet type counters are checked in the priority order shown in figure2.9. The packet type of the next packet is determined and used to decide which circular buffer to pop the packet data from. The data is sent from the circular buffer to the SPI buffer in preparation for sending to the SPORT spacecraft. Multiple circular buffers were used to eliminate the complexity of using one circular buffer with varying packet sizes.

2.5 Testing Concepts of the SWP

The USU SWP development and testing occurred in the electronics laboratory spaces at Utah State University's Center for Space Engineering. The test area, shown in figure 2.10, is setup with ESD protection, power supplies, and signal generators. A spacecraft emulator was used for testing the SPI communication interface and debugging. A Faraday cage with an internal thermal chamber were used for thermal testing. The SWP PCB was mounted to an internal cold/hot plate that was controlled by an external circulating fluid
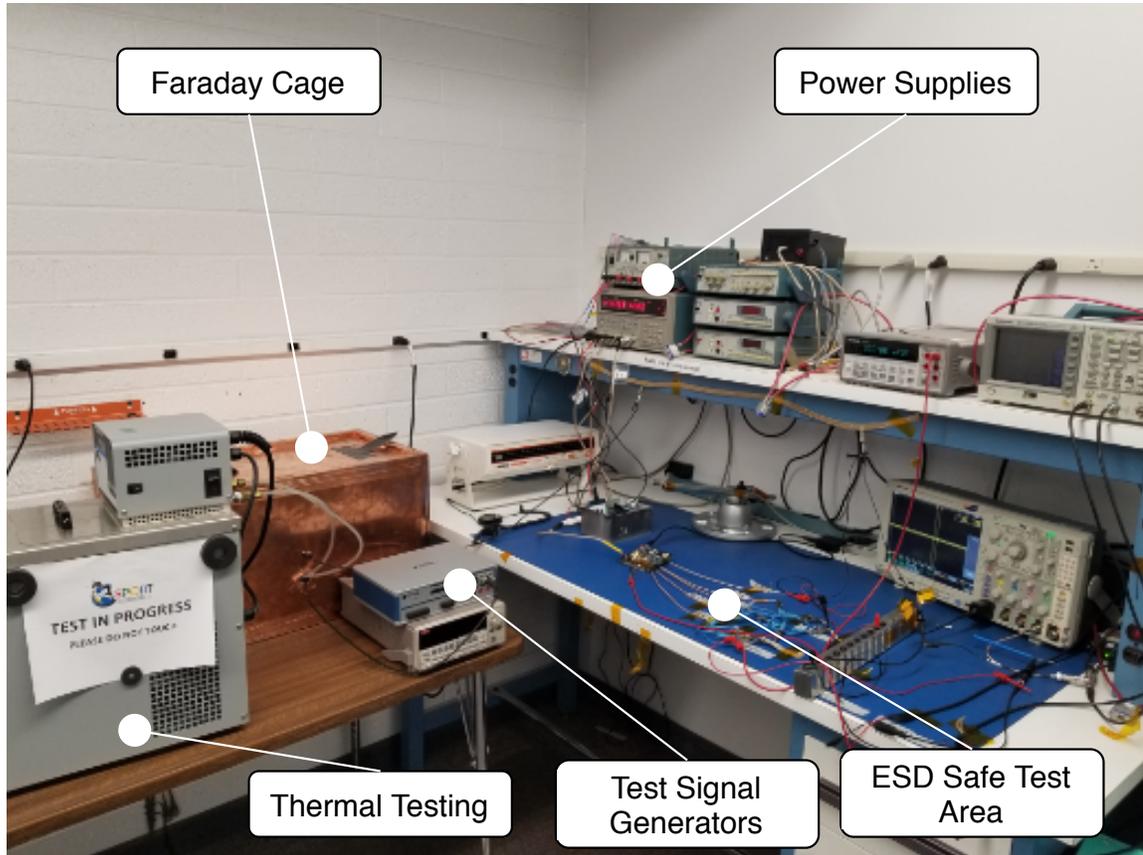
bath.

Fig. 2.10: USU SWP Testbench Setup

The SPORT spacecraft emulator consists of a Raspberry Pi computer with a GPS receiver and external hard drive. The software on the Raspberry Pi emulates the communications between the SWP and the SPORT spacecraft. The raw data received from the SWP is stored on the hard drive and sent to a COSMOS ground station via TCP/IP. The COSMOS ground station is used for sending commands via the emulator to the SWP and plotting data received from the SWP in real time. Test sources were used to inject signals into the SLP, EFP, and SIP. Figure 2.11 shows the test bench setup for the test sources used during calibration and testing of the USU SWP. Test sources were controlled via MATLAB and LabVIEW scripts. These scripts also control the data logging of the telemetry on the Raspberry Pi.
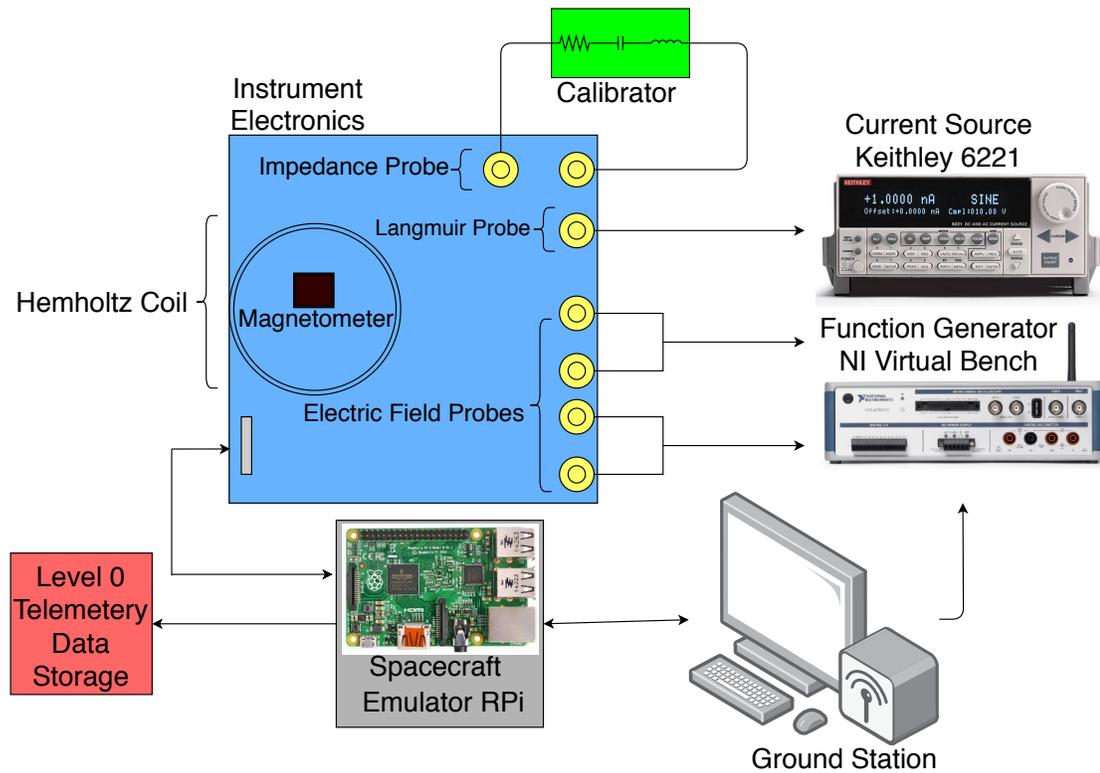
Fig. 2.11: Testbench Setup

2.6 Data Analysis Concepts

The data analysis concepts for of the USU SWP are illustrated in Figure 2.12 which overviews the process for converting the raw data into measurements of plasma density, electron temperature, and measurements of wave power in both density and electric field. The USU SWP produces various CCSDS Space Packets which contain data that is called Level 0 and consist of ADC counts, timing, and housekeeping information. The Level 0 data are processed into Level 1 data which in turn is processed into Level 2 data by using a series of MATLAB scripts and functions. The Level 0 ADC counts are calibrated into current, voltages, frequencies, and impedances using the calibrations computed during the thermal testing of the instrument. These become Level 1 data. The Level 1 data is also registered to GPS time and combined with ancillary data from the spacecraft, so the lighting, position, and orientation of the probes are known in both inertial and Earth Fixed reference frames. The level 1 data is then analyzed using the appropriate probe theory to produce the Level

2 data consisting of scientific measurements of density, temperature, wave power, magnetic and electric fields as a function of position and time. These are to be used by the science community for addressing the SPORT science questions. Level 2 data will be stored by EMBRACE at INPE and shared with the science community via the existing EMBRACE web portal.
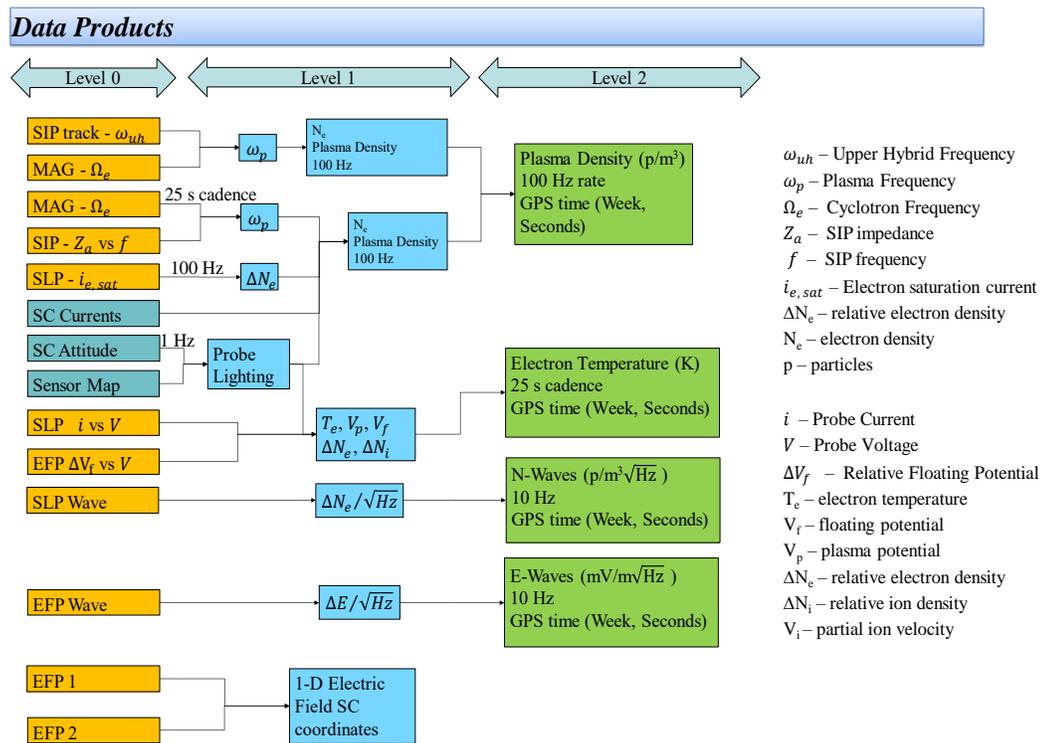

Fig. 2.12: Data Products

The primary measurement of the SWP is the plasma density along the spacecraft track at 100 Hz, or, given the spacecraft velocity of 7.66 km/s, at a spatial sampling of 76 meters. This density is computed using three separate techniques. The first and most direct path is to use the tracking data of the SIP which gives the upper hybrid frequency at 100 Hz. This is combined with measurements of the local magnetic field to obtain the plasma frequency from which plasma density is directly obtained. A second method is to use the frequency sweeps of the SIP and to manually locate the upper hybrid frequency in the probe current

vs frequency plots. This can only be done at the slow cadence of the SIP sweep which will be nominally operated at 25 to 120 second period. The SLP DC electron saturation current measurement is proportional to the electron density and sampled at 100 Hz but only provides a relative measurement of plasma density. Therefore, this relative measurement will be continually calibrated using the slower SIP sweeps to produce an absolute measurement at the required rate. The third method is the least accurate but produces an additional electron temperature parameter. This method relies on the SLP sweeps and probe theory, as well as the probe orientation and lighting, to compute the absolute electron density, temperature, as well as the ion density. These will then be used to calibrate the SLP DC electron saturation current to produce a 100 Hz plasma density measurement.

The SWP produces a Level 2 data product that is the measurement of both electron density and electric field wave power. The source of the electron density wave power data originates from the SLP DC electron saturation current measurement and the electric field wave power originates from the electric field probes. The powers are determined from the L1 data by applying the ground-based calibrations to each of the 16 frequency bands stretching from 25 Hz to 25 kHz and in the case of the electron density, wave power, using the SIP relative calibration to electron density. The final measurement of interest is a one dimensional observation of the electric field as determined by the difference between the two floating probe measurements. This is not reported as a Level 2 data product but will be used for comparison internal to the SPORT mission with the electric fields as determined from the UTD drift meter.

CHAPTER 3

SWEEPING LANGMUIR PROBE

Langmuir probes have been used for many years as a method for in-situ measurement of plasma characteristics. The probes have been flown on both sounding rockets and satellites. [1] This thesis focuses on miniaturizing the instrument for use on a CubeSat and therefore will not go into large detail on instrument theory. For a more detailed tutorial of the theory of Langmuir probes, see *Langmuir Probe Measurements in the Ionosphere* [10].

3.1 Instrument Overview

A Langmuir probe consists of a metal conductor immersed in a plasma and a voltage is applied to the probe. The resulting current collected on the probe is measured. This measurement allows for the I-V curve of the plasma to be determined when the voltage is swept through a range of values as seen in Fig. 3.1
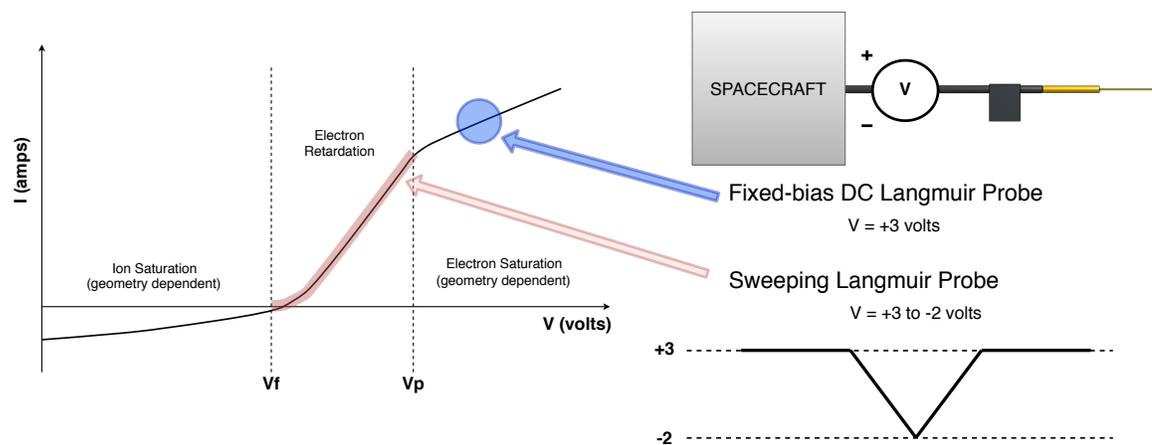

Fig. 3.1: IV Curve Langmuir Probe

Fig. 3.2: Location of SLP analog components on the USU SWP PCBA

From this curve, several plasma parameters including electron density, ion density, and total electron temperature can be obtained due to proportional relationships with the currents measured. The ion current I_i is proportional to the ion density, N_i. There is also a proportional relationship between the electron current, I_i and electron density, N_e. The DC probe measures collected current in the saturation region. This measurement is done by applying a fixed voltage potential relative to the spacecraft ground. The Sweeping probe measures collected current at each step of a voltage sweep. Both the DC and Sweeping probe are affected by changes in the spacecraft floating potential. To account for this shift, floating potential probes are used to monitor the spacecraft floating potential during operation of the Langmuir probe. The implementation of the SLP is designed to use less power and area than previous implementations. The SLP is a combination of an analog front end and digital components implemented in FPGA fabric. There are two channels for the SLP, a low gain and high gain channel. The USU SWP Langmuir Probe has two possible operating modes, DC (Fixed-bias) and Sweeping. Both modes utilize the same analog front end but differ in the digital components.

3.2   Design and Analysis

3.2.1 Instrument Requirements

In order to meet the SPORT science requirements, it was determined that the Sweeping Langmuir Probe would need to be designed to meet the Functional requirements shown in Table 3.1. The test range used to verify each of these requirements is also shown. More detail on the testing is provided in the Calibration and Testing section at the end of this chapter.

Table 3.1: Key SLP Functional Requirements

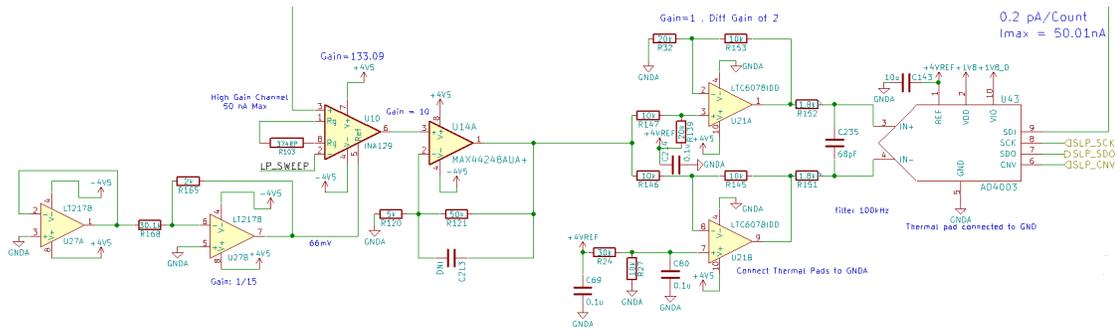| Parameter	Units	Requirement	Test Range
Output Voltage Range	Volts	-2 to +3	-3 to +3
High Gain Current Range	na	-50 to +50	-55 to +55
Low Gain Current Range	uA	-50 to +50	-55 to +55
Measurement Bandwidth	Hz	> 40	1 to 50
Sweep Step Sample Rate	Hz	> 2000	20,000

3.2.2 Analog Design

The SLP consists of an analog front end shared by both channels with a transimpedance amplifier (TIA), that measures the input current on the probe. The chosen TIA, LTC2057, is a low noise, zero-drift amplifier with low offset voltage drift from temperature. The amplifier output V_{out} is determined by the equation below where I_{in} is the current into the TIA, G is the gain of the amplifier, V_{bias} is the voltage on the probe.

$$I_{in} * G_{tia} + V_{bias} = V_{out} \tag{3.1}$$

$$(V_{out} - V_{bias}) * G_{diff} = V_{diff} \tag{3.2}$$

The next stage takes V_{diff} and converts it into a differential signal to drive the ADC. The input to the ADC is centered around $V_{ref}/2$. The ADCs are 20 bits, with $2^{20}/4.096$ counts per volt.
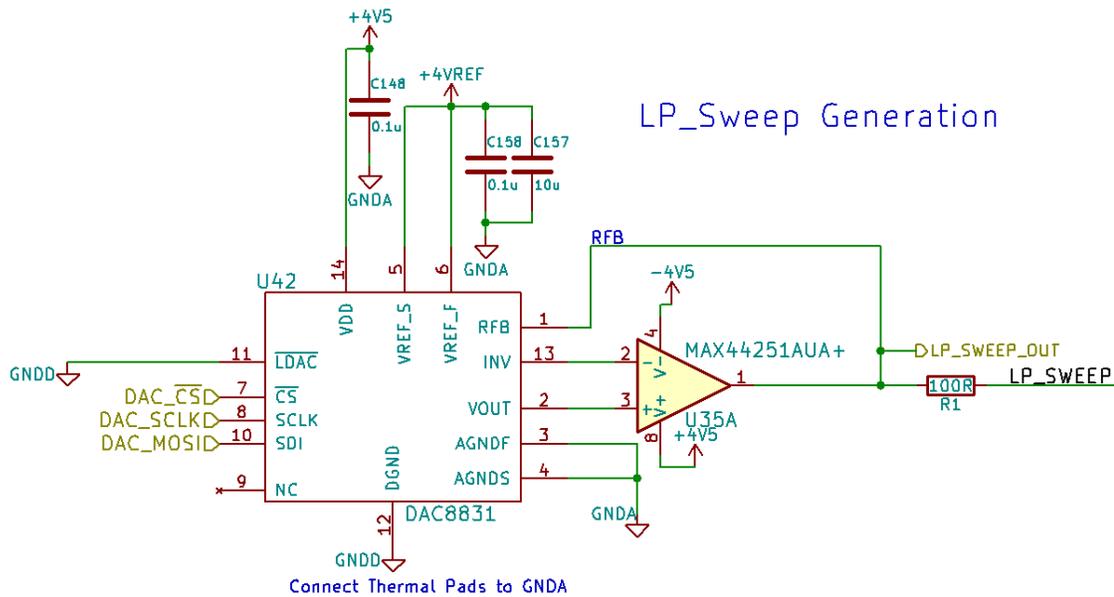
Fig. 3.4: Sweeping Langmuir Probe High Gain Channel

Fig. 3.3: Sweeping Langmuir Probe Low Gain Channel

V_{bias} is produced by a DAC paired with an operational amplifier for bipolar output operation. The DAC8831 is an ultra-low power, low-noise DAC, with a fast settling time. The MAX44251 is an ultra-precision, low-noise, low-drift amplifier. This op-amp was chosen due to its near zero DC offset and low thermal drift. The DAC is controlled by a driver on the FPGA using SPI to send voltage values. The DAC produces a fixed voltage during DC mode and uses a look up table for the voltage sweeps during Sweep mode. The DAC is 16 bits with a resolution of 125uV/count.

3.2.3   Digital Design

The digital section of the SLP is implemented in the fabric of the Microsemi Smartfusion 2 FPGA. The FPGA architecture is shown in figure 2.5. A SPI interface is used between the ADCs and FPGA fabric. To reduce the number of FPGA pins used, the two SLP ADCs are used in a daisy chain configuration. Daisy chain configuration allows for a reduction of

Fig. 3.5: Sweeping Langmuir Probe DAC

FPGA pins by sharing one SDO pin with multiple ADCs. The SDO from one ADC is tied to the SDI of the next. The final ADC's SDO is tied to the input of the FPGA. The FPGA clocks the data for all the ADC's on the chain consecutively with each read.

The SLP Low gain and High gain ADCs sample period is configured using an adjustable ADC sample timer. The sample timer triggers the SPI drivers to send a conversion command to the ADCs by asserting the CNV line. A sample is ready from the ADC after a delay of t_{conv}, which is a max of 320 ns. The SPI driver now clocks the sample data from the ADC. When the sample data is received, the accumulator WEN signal is asserted, allowing the accumulators to register the data from the SPI driver. The DC and Sweep channels have separate banks of identical accumulator modules. The accumulators act as low pass filters on the Langmuir probe measurements. Each accumulator waits for a trigger to register the data on the input. There are two adjustable parameters for the accumulator, the number of samples to skip and the number of samples to sum. Skipping samples provides the ability to allow for a settling time on each step of the sweep. This can be seen in figure Fig. 3.7, where two ADC samples occur while the DAC voltage is still settling.
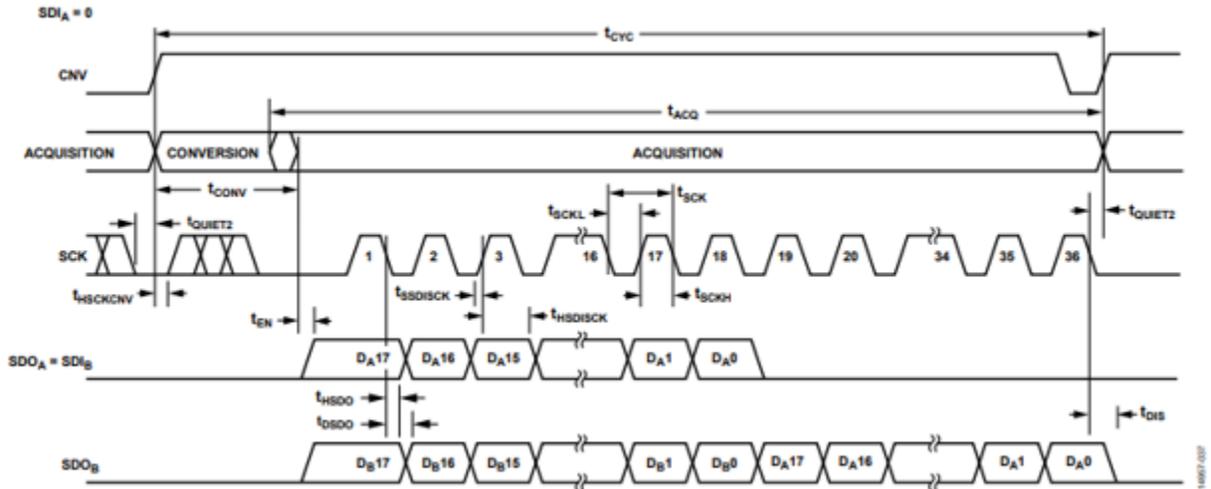
Fig. 3.6: Timing Diagram for daisy chained ADC from AD4003 Datasheet
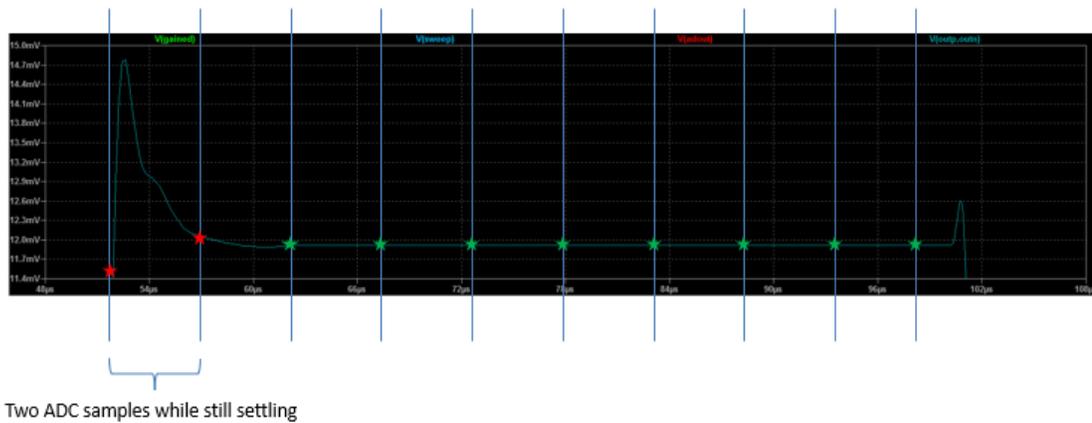

Two ADC samples while still settling

Fig. 3.7: DAC settling time and ADC samples

Once the desired number of skipped samples, M, have been discarded, the accumulator begins to save and sum each ADC sample. After the accumulator has summed the required number of samples, N, the accumulator's DONE signal is asserted. The accumulator resets on the next clock cycle.
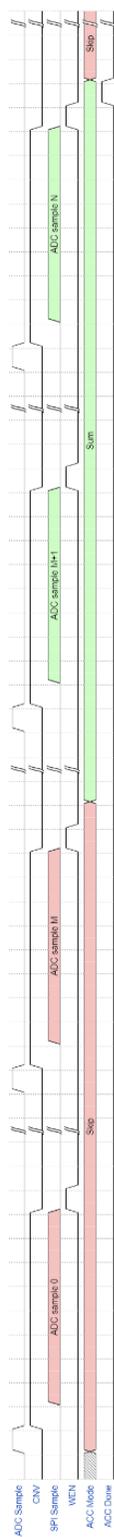
Fig. 3.8: SLP Sample timing

The Gather and Mask module receives all the data from the accumulators. The Gather and Mask modules have an adjustable shift parameter, which allows for averaging and selecting what bits of the accumulator output are used. When each accumulator is done, the data is saved in a register until all accumulators have been read from. At this point the DC channel Gather and Mask triggers a magnetometer conversion and reads the current SysClock value. When a packet granule is ready, which includes all accumulator data, the magnetometer data, and the SysClock, the granule is fed word by word into the FIFO. The FIFO asserts the AFULL flag once a complete granule is stored. The AFULL flag triggers an interrupt in the microprocessor. The microprocessor then reads the granule out of the FIFO over the APB. The FIFO can store a full telemetry packet's worth of granules in the event that the microprocessor is delayed in reading out a granule. The DC and Sweep channels can be operated independently. However, if both channels are operating simultaneously, the DC data obtained during a Sweep should be considered unusable. The Sweep mode of the SLP uses a sweep timer to determine the period between sweeps. The SLP Sweep Timer also determines the length of each sweep. The sweep timer module counts the number of ADC samples at each step and triggers the step changes. At each step of the sweep, the sweep timer sends an address to the SLP Sweep Table module. The table module reads the step value out of RAM which is then used to set a voltage on the probe guard by the SLP DAC driver. The EFP ADCs are sampled simultaneously with the SLP ADCs. The same data processing chain is used for the EFP samples. The EFP provides the floating potential measurements discussed at the beginning of this chapter.
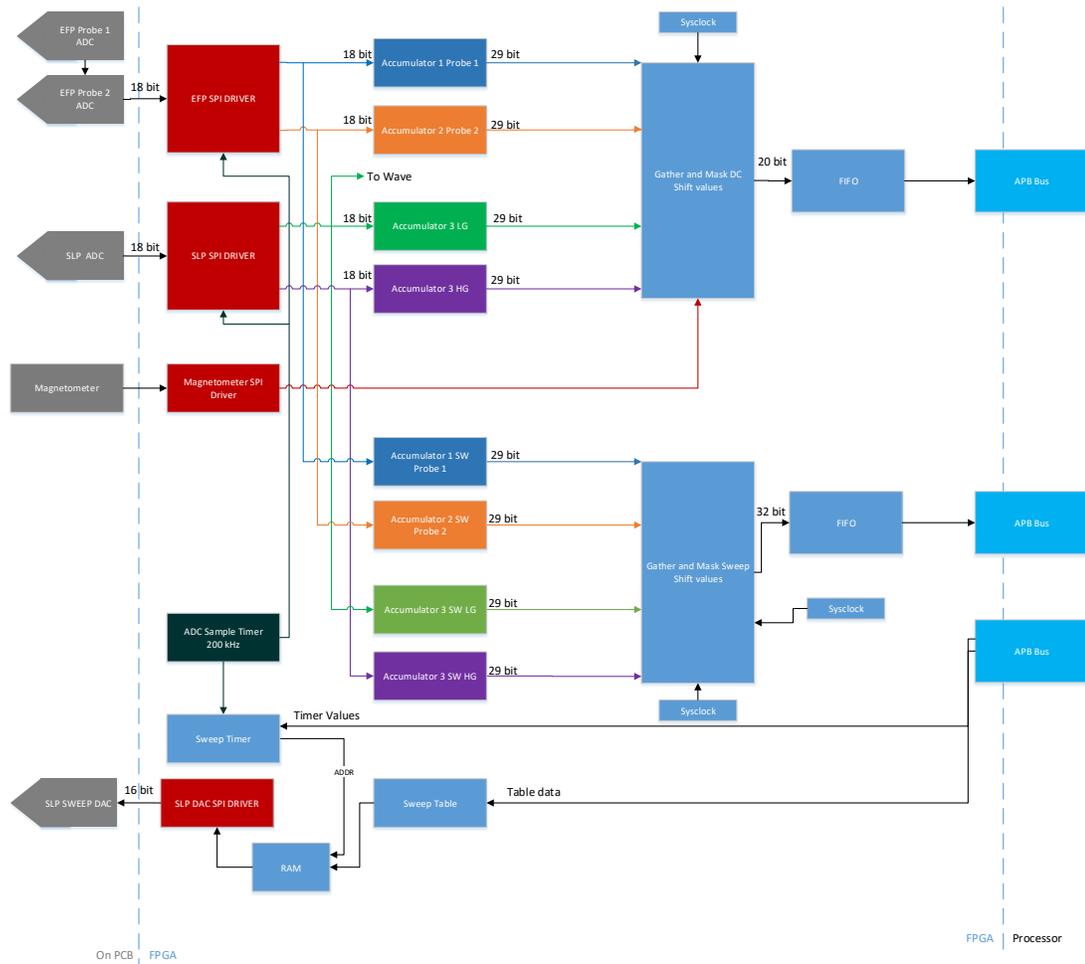
Fig. 3.9: FPGA flow diagram for SLP/EFP

3.3   Calibration and Testing

The Sweeping Langmuir Probe was subjected to a number of test to determine if the instrument meets the functional requirements in Table 3.1 All tests were conducted over a thermal range as shown in figure 4.6
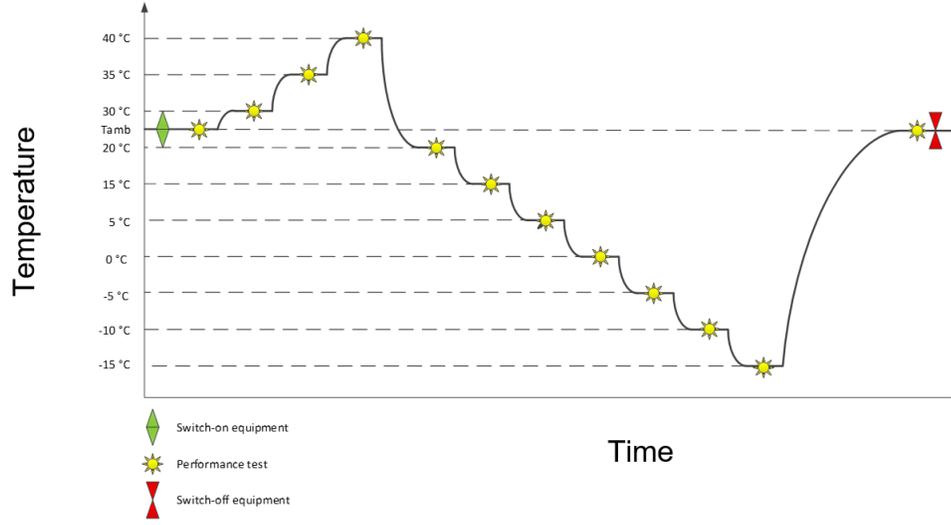
Fig. 3.10: Thermal cycling concept

3.3.1 Calibration Methodology

Gain and Linearity Test with Current Source

The purpose of this test was to determine the gain and offset of the Langmuir probe over the temperature range and check the linearity of the instrument. The first test was conducted by driving a known current into the SLP using a current source. The DAC is set at minimum voltage, zero voltage, and maximum voltage for the probe. The current range for the High and Low gain channels was verified with a stepped input current. Figure 3.13 shows the results from the Linearity test. Figure 3.14 gives the calibration obtained using the test data. $SLP_{LG} = -2.0165e^{-04} \cdot ADC + 0.3449$ The test results across the range of temperatures were compared and figure 3.15 shows how the calibration changed with temperature.
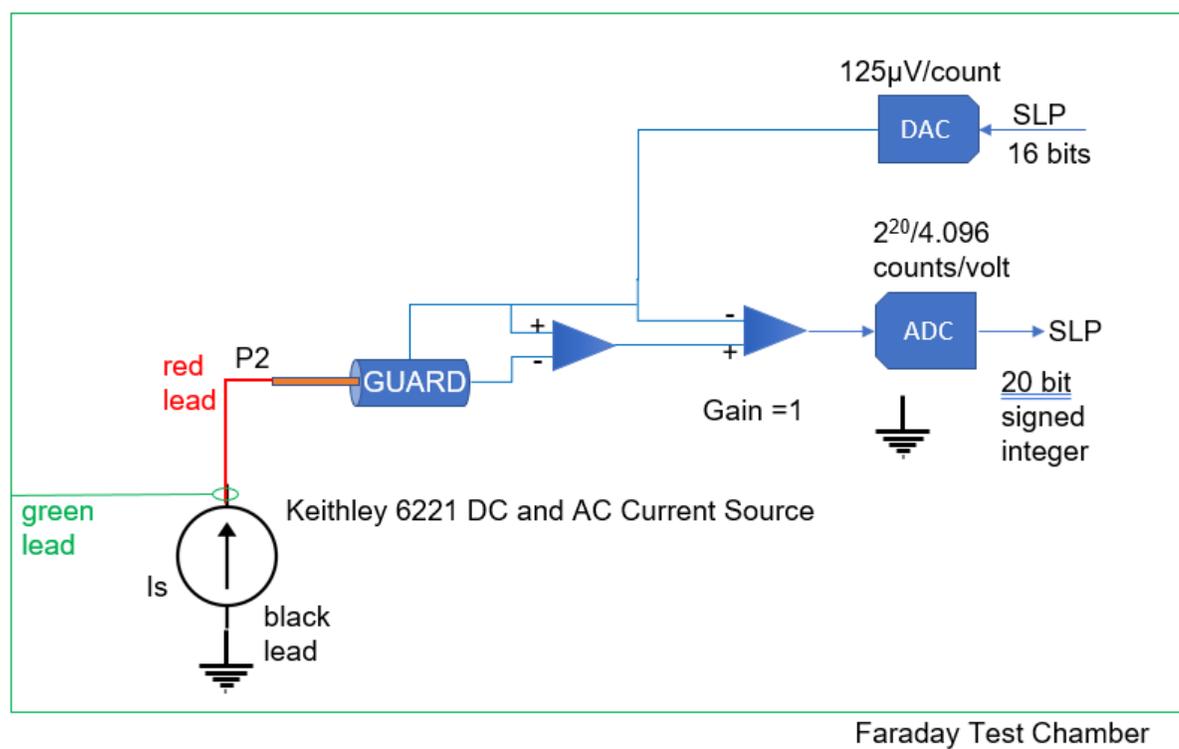
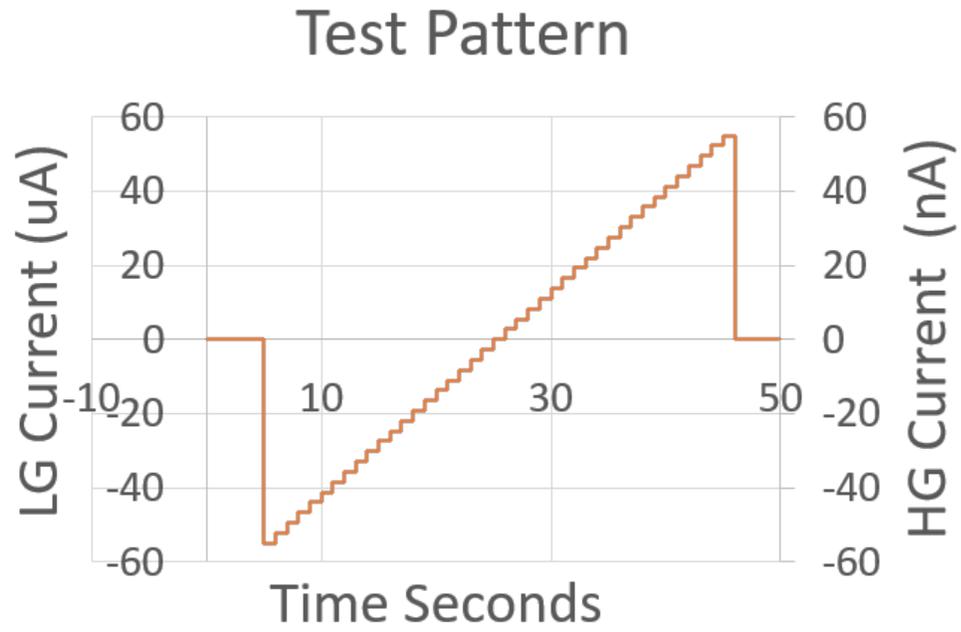Fig. 3.11: SLP Test setup with current source

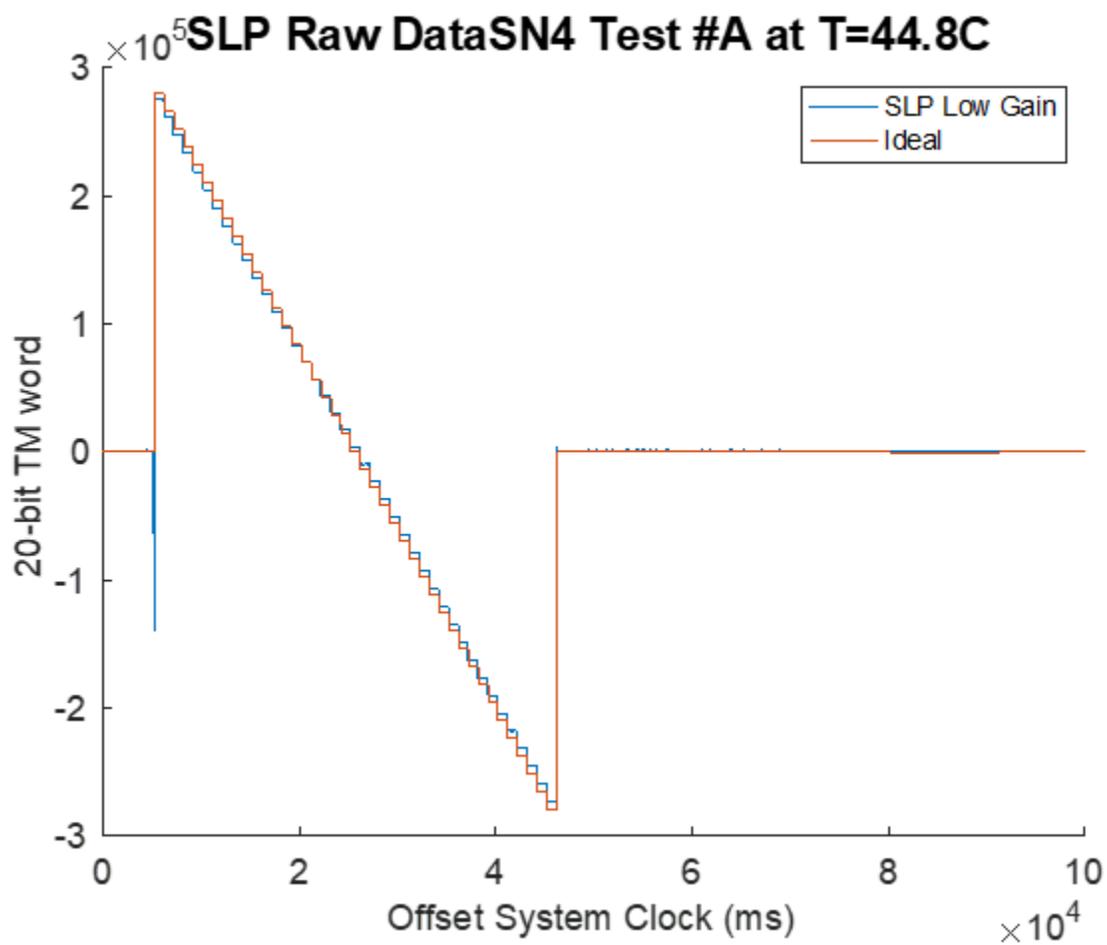Fig. 3.12: SLP Gain and Linearity Test input current pattern

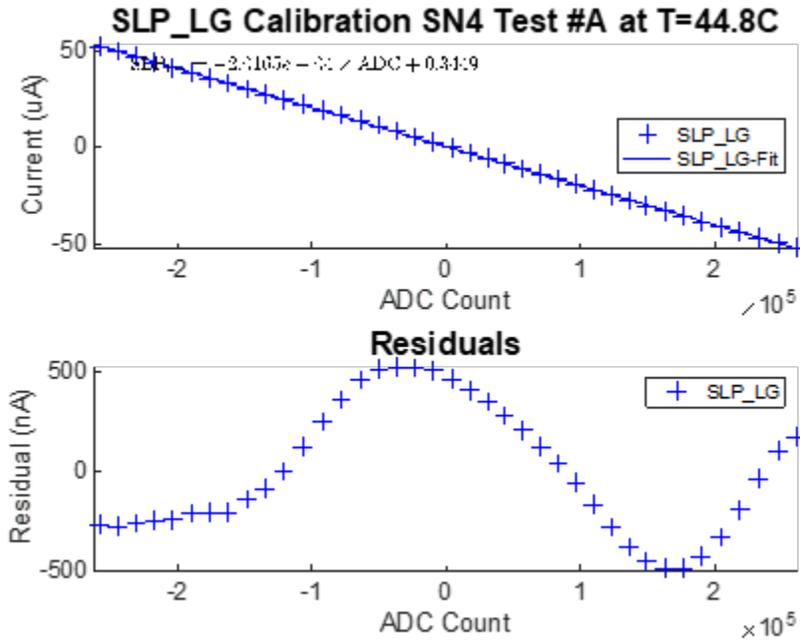Fig. 3.13: Results of Gain and Linearity Test with Current Source
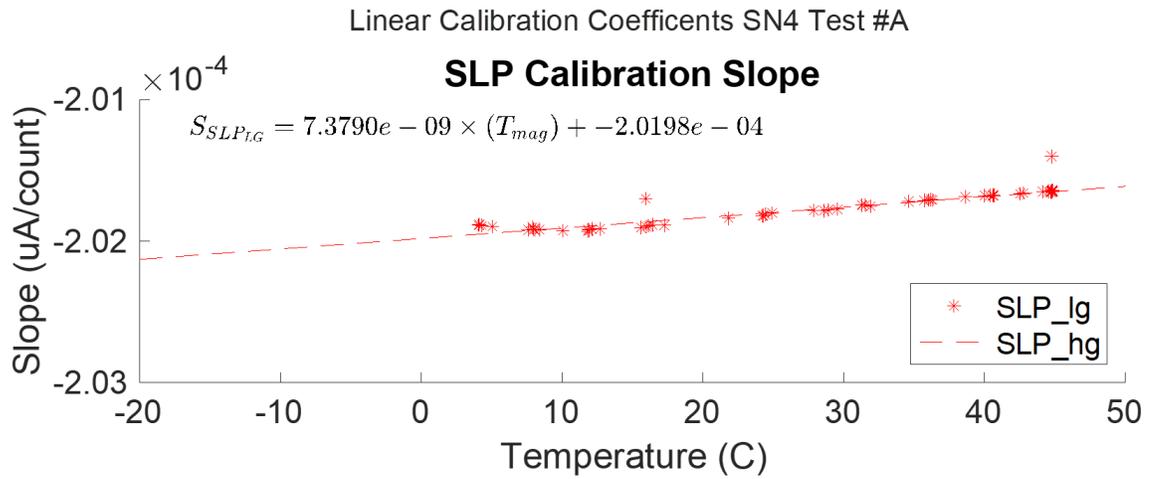
Fig. 3.14: SLP Calibration

Fig. 3.15: Calibration vs Temperature

Gain and Linearity Test with Precision Resistors

The purpose of this test was to determine the gain and offset of the Langmuir probe
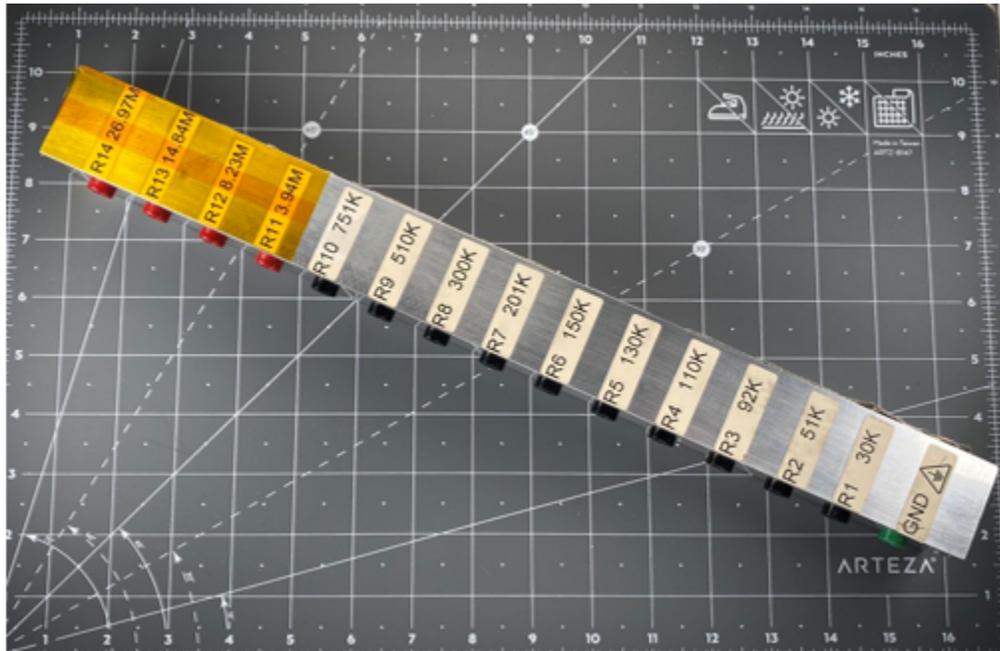
Fig. 3.16: SLP Precision Test Resistors

over the temperature range and check the linearity of the instrument. This second test was conducted using finely calibrated resistors across the SLP to determine the gain and linearity with more precision.

Table 3.2: Precision Resistor values with expected current and ADC counts

Resistor	Value (k ohm)	Current (uA)	LG Count
R1	30	100	5.24E+05
R2	51	58.8	5.24E+05
R3	92	32.6	3.42E+05
R4	110	27.3	2.86E+05
R5	130	23.1	2.42E+05
R6	150	20.0	2.10E+05
R7	201	14.9	1.57E+05
R8	300	10.0	1.05e+05
R9	510	5.9	6.17E+04
R10	751	4.0	4.19E+05
R11	3945	0.8	7.97E+05
R12	8237	0.4	3.82E+03
R13	14843	0.2	2.12E+03
R4	26971	0.1	1.17E+03

SLP Frequency Response

The purpose of this test was to determine the frequency response of the Langmuir probe over the temperature range. Sine waves were input to the SLP over the frequency range shown in table 3.3.

Table 3.3: SLP Frequency Steps

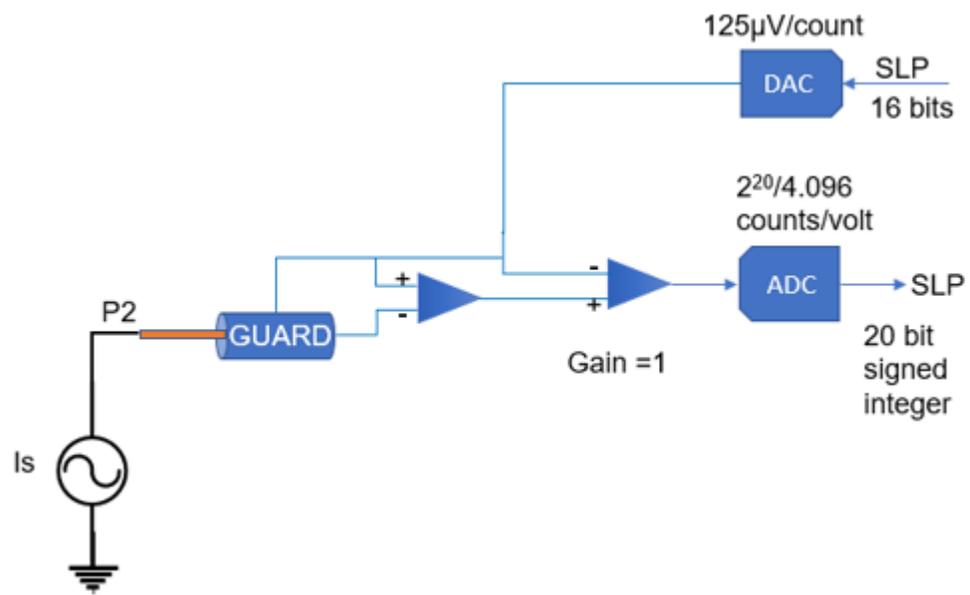| Point	Frequency (Hz)	Hold (s)	Point	Frequency (Hz)	Hold (s)
1	5	20	31	417	1
2	6	17	32	484	1
3	7	15	33	560	1
4	8	13	34	649	1
5	10	10	35	752	1
6	11	10	36	872	1
7	13	8	37	1010	1
8	15	7	38	1171	1
9	17	6	39	1357	1
10	19	6	40	1572	1
11	22	5	41	1822	1
12	26	4	42	2111	1
13	30	4	43	2447	1
14	34	3	44	2835	1
15	40	3	45	3286	1
16	46	3	46	3808	1
17	53	2	47	4413	1
18	62	2	48	5114	1
19	72	2	49	5926	1
20	83	2	50	6867	1
21	96	2	51	7958	1
22	111	1	52	9223	1
23	129	1	53	10688	1
24	149	1	54	12386	1
25	173	1	55	14353	1
26	200	1	56	16634	1
27	232	1	57	19276	1
28	268	1	58	22339	1
29	311	1	59	25888	1
30	360	1	60	30000	1

Fig. 3.17: SLP Frequency Response Test setup

CHAPTER 4

ELECTRIC FIELD PROBE

4.1 Instrument Overview

Electric Field Probes fundamentally are voltmeters measuring the electric potential between the probe and spacecraft body. The EFP probe tips are deployed X cm from the spacecraft body and float to a potential relative to the ionospheric plasma. The EFP allows for locating the floating potential shown on the I-V curve as seen in Fig. 4.1 when used in conjunction with the Langmuir Probe.
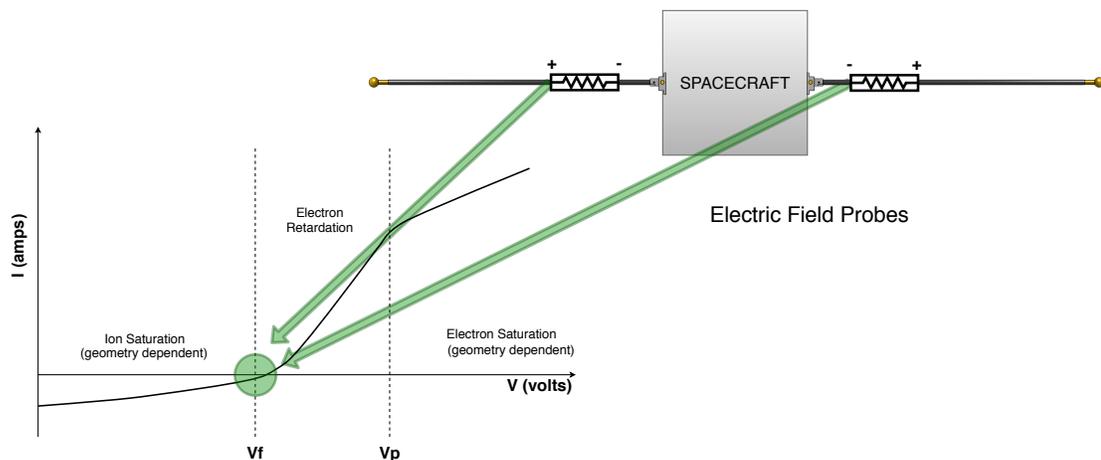

Fig. 4.1: IV Curve Electric Field Probe

The EFP is also used to measure DC and AC electric fields. [11] Further information on the operational theory of Electric Field Probes in a plasma can be found in *Design, Test, And Calibration of the Utah State University Floating Potential Probe* [6].

4.2 Design and Analysis

Fig. 4.2: Location of EFP analog components on the USU SWP PCBA

4.2.1 Instrument Requirements

To meet the SPORT science requirements, it was determined that the Electric Field Probe would need to be designed to meet the Functional requirements shown in Table 4.1. The test range used to verify each of these requirements is also shown. More detail on the testing is provided in the Calibration and Testing section at the end of this chapter.

Table 4.1: Key EFP Functional Requirements

Parameter	Units	Requirement	Test Range
Input Voltage Range	Volts	-1.7 to +1.7	-1.9 to +1.9
Measurement Precision	uV	< 360	TBD
Measurement Bandwidth	Hz	40	50
Input Resistance	Ohms	$R > 10^{10}$	$R > 10^{11}$

4.2.2 Analog Design

The EFP consists of two sensors deployed from the spacecraft. The design builds on

the EFP used on the ASSP mission. For more information on the EFP design, refer to the ASSP thesis. /citeFarr-ASSP The Electric field instrument has two analog channels, one for each probe as seen in figure 4.3
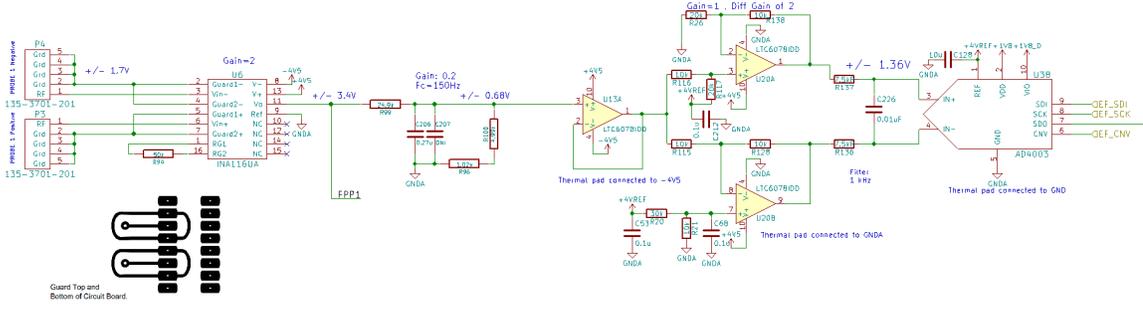

Fig. 4.3: Electric Field Probe 1 Channel

The input of each channel has an instrumentation amplifier (IA). The INA116 from Texas Instruments, shown in figure 3.3, was chosen due to its extremely low input bias current. The inputs to the INA116 are shielded with driven guards to maintain the extremely low input bias current. The voltage output of the IA is given by equation 3.1 with a gain determined by equation 3.2.

$$V_{IA} = (V_{in+} - V - in-) * G \tag{4.1}$$
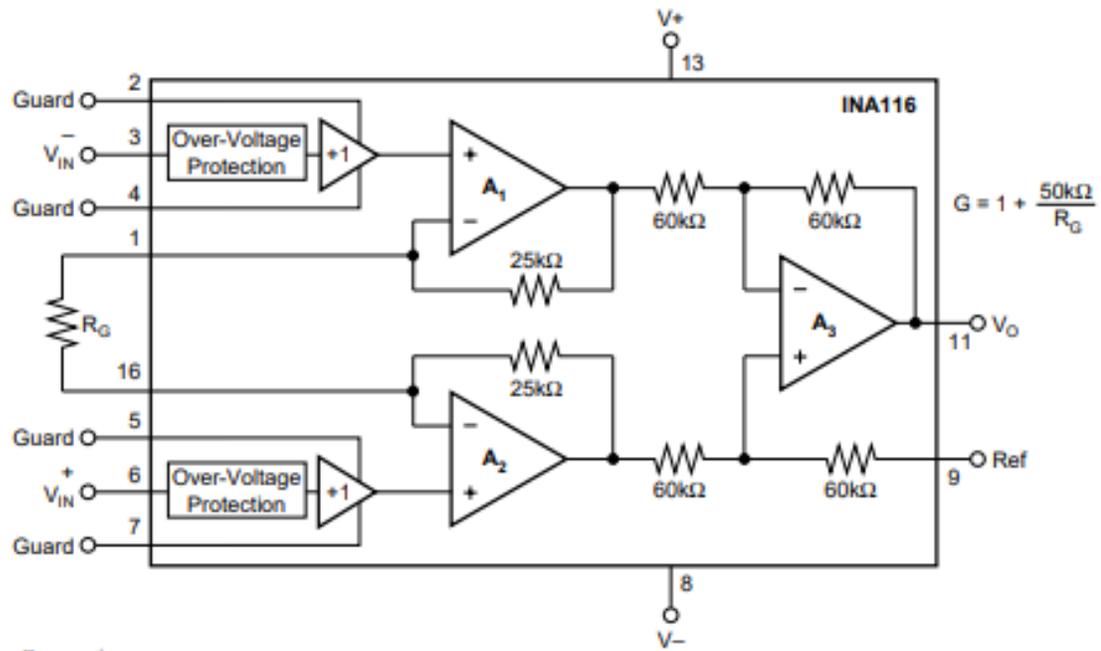
$$G = 1 + \frac{50k\Omega}{R_G} \tag{4.2}$$

Fig. 4.4: EFP INA116 Instrumentation Amplifier Diagram from INA116 Datasheet

4.2.3 Digital Design

The EFP shares the same digital processing as the SLP previously discussed in Chapter 2, section 2.2. The digital gain of the EFP can be adjusted independently from the SLP.
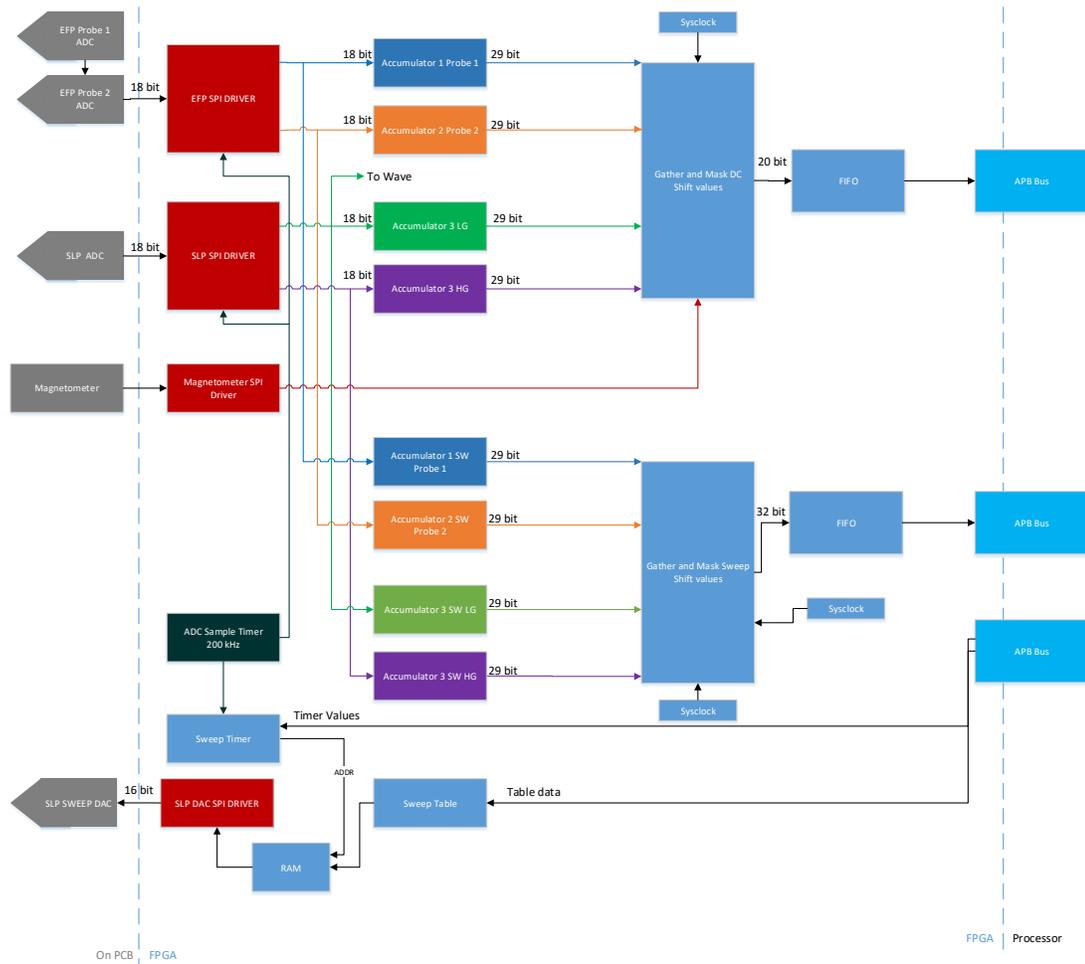
Fig. 4.5: FPGA flow diagram for SLP/EFP

4.3 Calibration and Testing

The Electric Field Probe was subjected to a number of test to determine if the instrument meets the functional requirements in Table 3.1 All tests were conducted over a thermal range as shown in figure 4.6
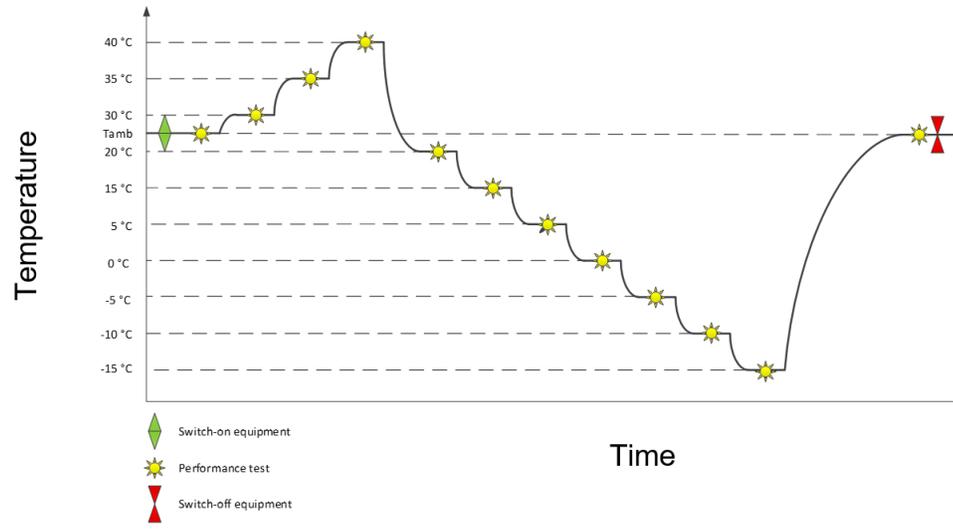
Fig. 4.6: Thermal cycling concept

4.3.1 Calibration Methodology

EFP Gain and Offset

The purpose of this test was to determine the gain and offset of the Electric Field instrument over the temperature range and to check the linearity of the instrument.
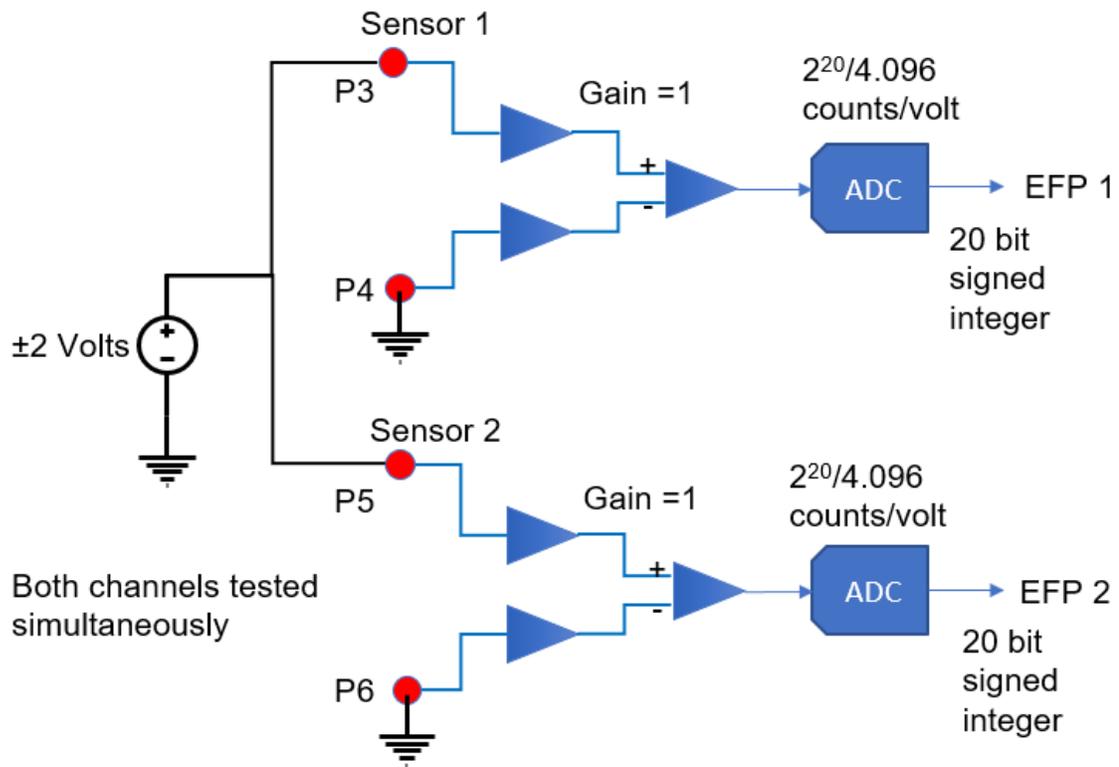
Fig. 4.7: EFP Gain and Offset Test Circuit

DC voltages were applied to the probes in a test pattern as shown in figure 4.7. The voltage is first held at 0 volts for 5 seconds. The voltage is then stepped from -2 to 2 volts in 0.1 volt steps with 1 seconds dwells. The test pattern is concluded with a hold at 0 volts for 4 seconds. Figure 4.9 shows the EFP output from the gain and offset test. The calibration obtained from the test results is shown in figure 4.10. The gain and offset over the range of tested temperatures is shown in figure 4.11.
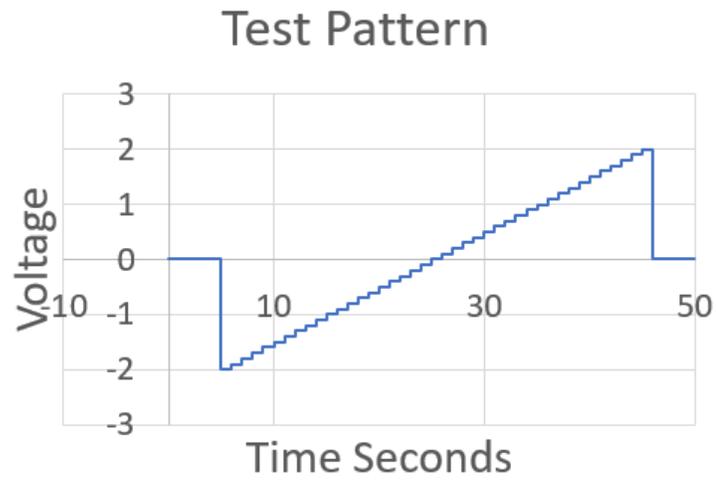
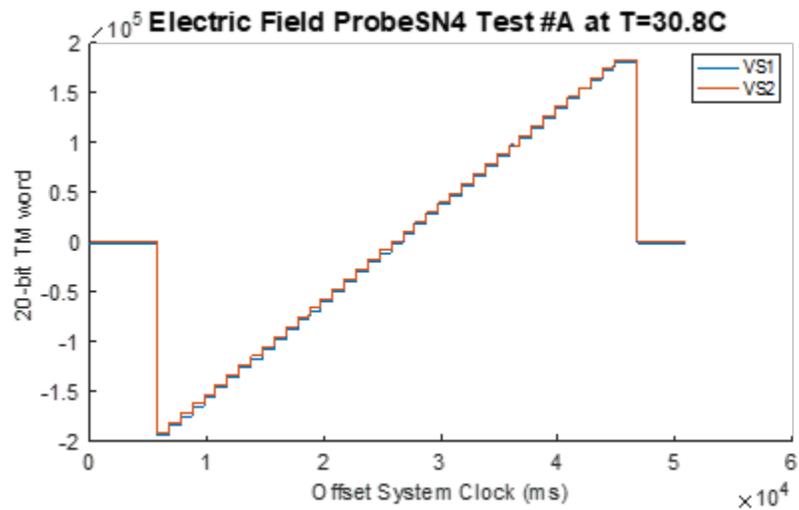Fig. 4.8: EFP Gain and Linearity Test input voltage pattern

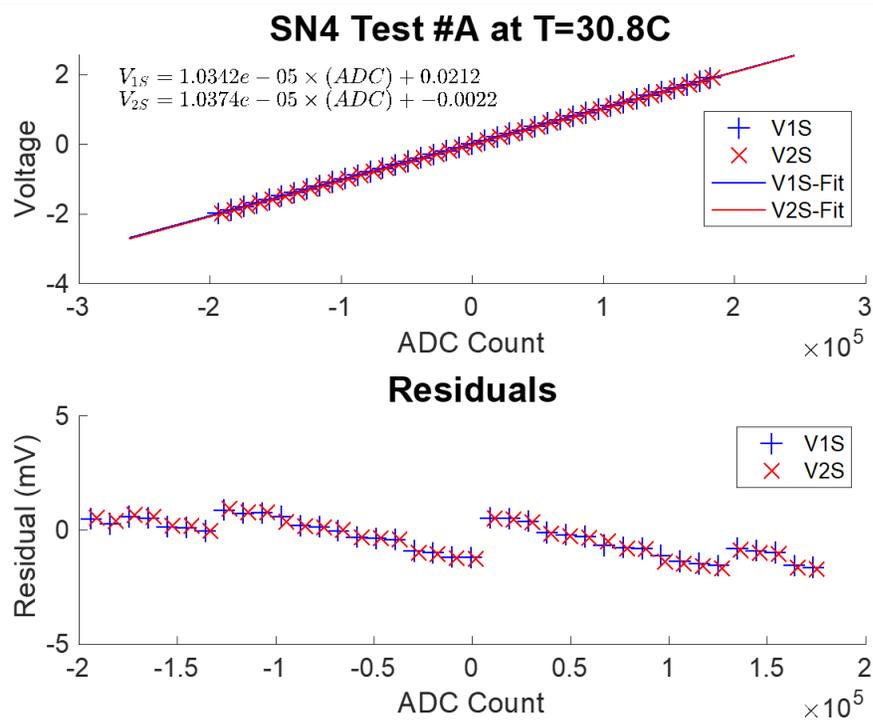Fig. 4.9: EFP Gain and Offset Test Output

Fig. 4.10: EFP Gain Calibration
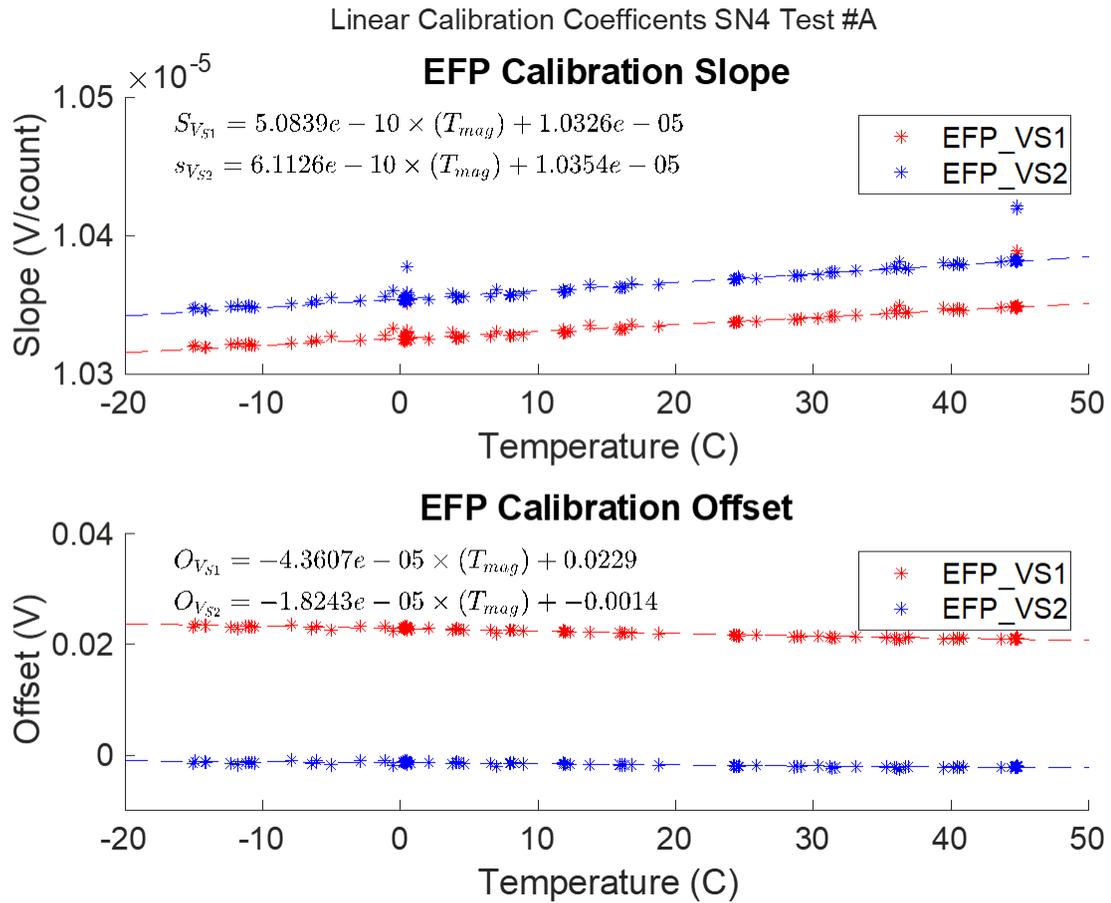
Fig. 4.11: Gain and Offset vs Temperature

EFP Frequency Response

The purpose of this test was to determine the frequency response of DC Electric Field instrument over the temperature range and to check the linearity of the instrument. Sinusoidal voltages were applied in steps to the probes as shown in the test setup in figure 4.12 using the National Instruments Virtual Bench. The frequency steps used for the test are given in table 4.2

Fig. 4.12: EFP Frequency Response Test Circuit

Table 4.2: EFP Frequency Steps

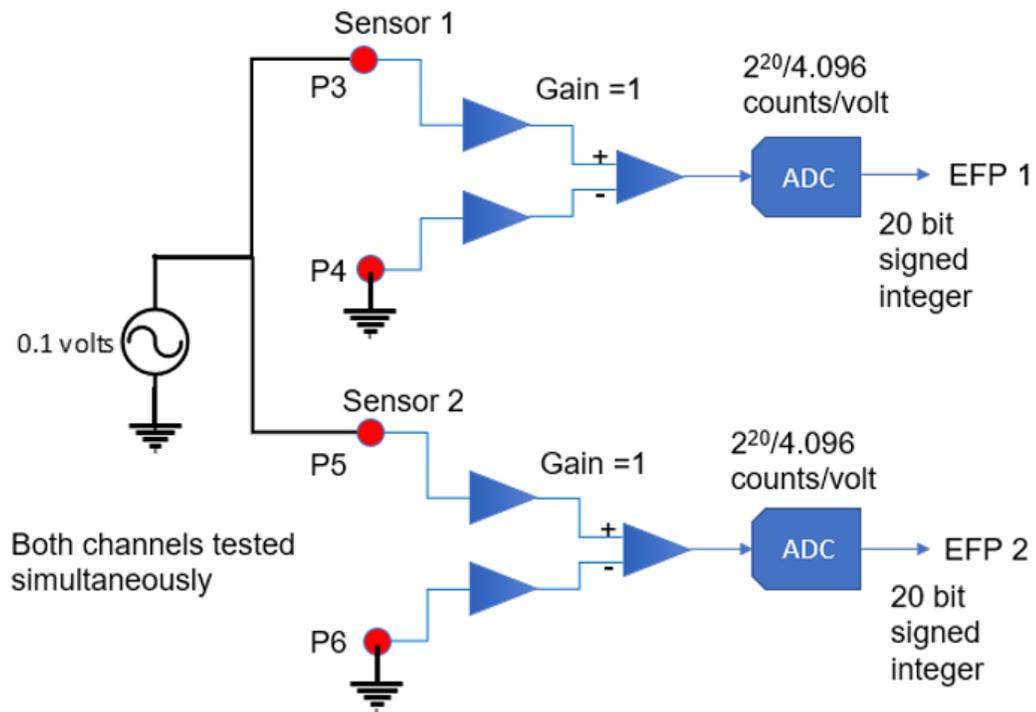| Point	Frequency (Hz)	Hold (s)	Point	Frequency (Hz)	Hold (s)
1	5	20	31	417	1
2	6	17	32	484	1
3	7	15	33	560	1
4	8	13	34	649	1
5	10	10	35	752	1
6	11	10	36	872	1
7	13	8	37	1010	1
8	15	7	38	1171	1
9	17	6	39	1357	1
10	19	6	40	1572	1
11	22	5	41	1822	1
12	26	4	42	2111	1
13	30	4	43	2447	1
14	34	3	44	2835	1
15	40	3	45	3286	1
16	46	3	46	3808	1
17	53	2	47	4413	1
18	62	2	48	5114	1
19	72	2	49	5926	1
20	83	2	50	6867	1
21	96	2	51	7958	1
22	111	1	52	9223	1
23	129	1	53	10688	1
24	149	1	54	12386	1
25	173	1	55	14353	1
26	200	1	56	16634	1
27	232	1	57	19276	1
28	268	1	58	22339	1
29	311	1	59	25888	1
30	360	1	60	30000	1

EFP Input Resistance

The purpose of this test was to demonstrate that the DC input resistance of the electric field probe is greater than the required threshold of 10^{10} Ohms. Figure shows the expected responses and the threshold required to meet the DC input resistance requirement.
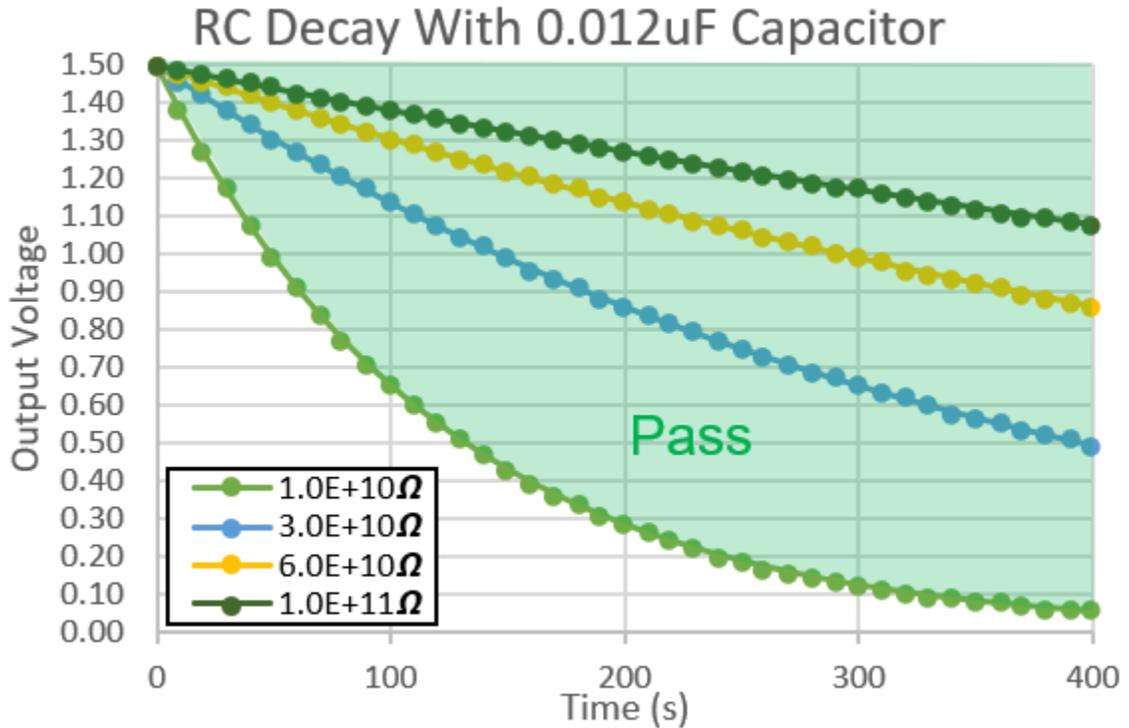

Fig. 4.13: Expected RC delay of calibration capacitor

A calibration resistor of 0.012 uF was used to observe the voltage delay when charged and the input shunted to ground. First, sensor 1 was connected to the capacitor and sensor 2 grounded. The capacitor was charged to +1.5 volts and the test repeated at -1.5 volts. Next, the setup was switched with sensor 2 connected to the capacitor and sensor 1 grounded and the tests repeated. The input resistance of the Electric field probe is given by equation 3.3.
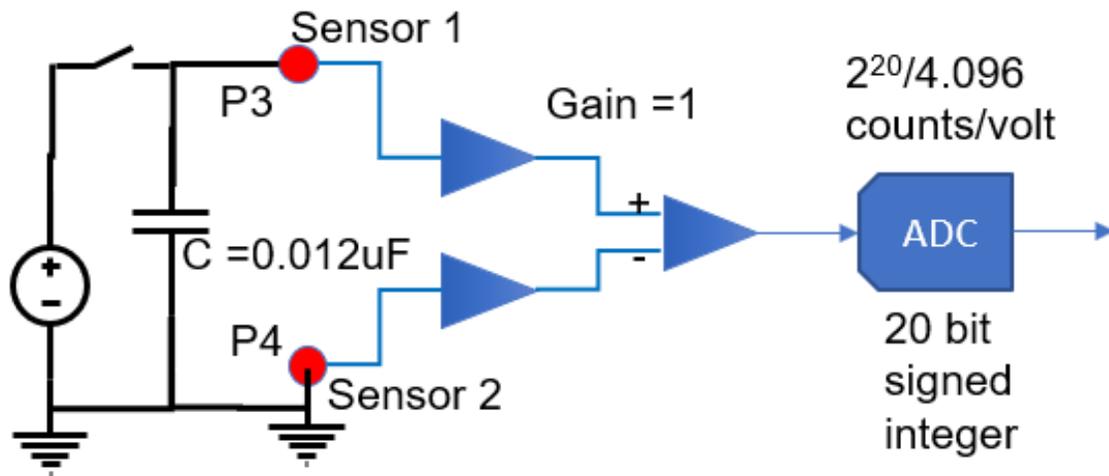
$$R = \frac{\tau}{0.012x10^{-6}} \tag{4.3}$$

Fig. 4.14: EFP Input Resistance Test Circuit

The results for this test are shown in figure 4.15. From the results we can see that the minimum input resistance threshold requirement is satisfied.
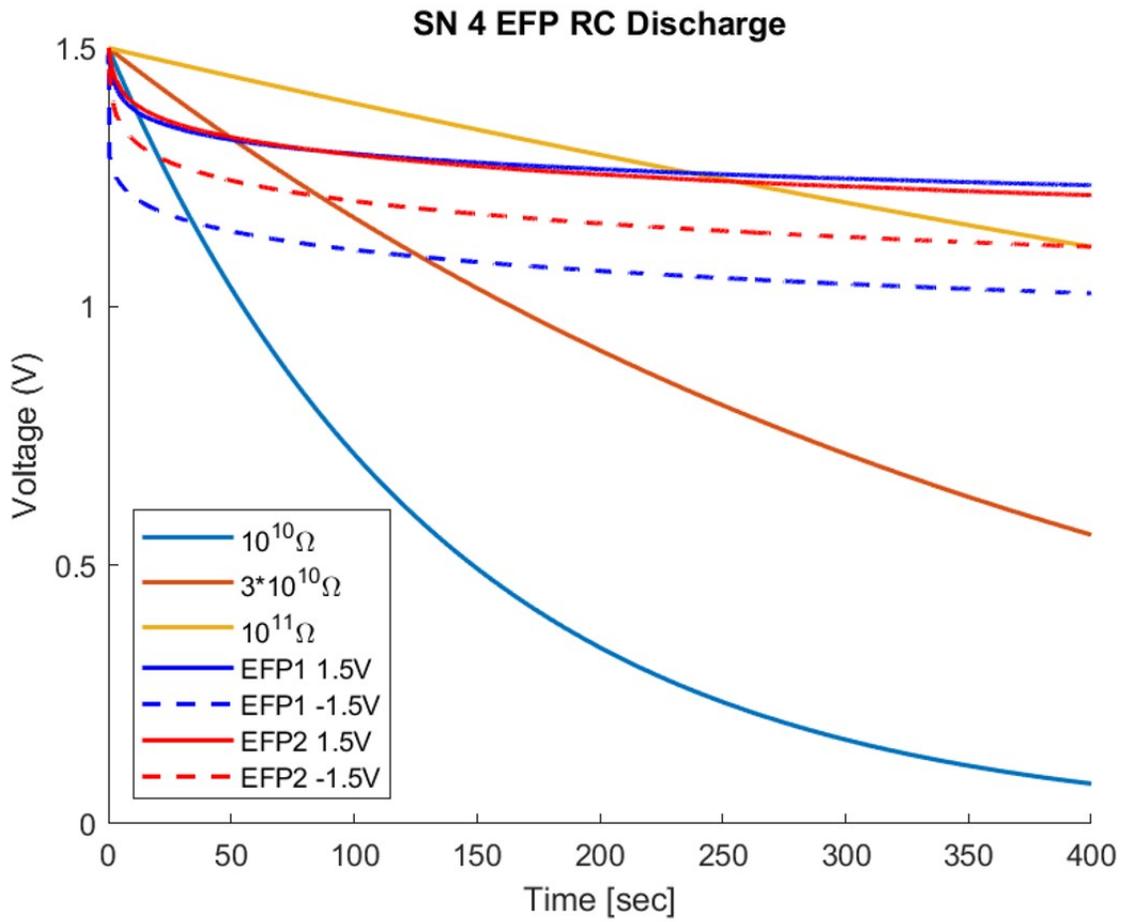
Fig. 4.15: EFP Input Resistance results for board SN4

CHAPTER 5

WAVE SPECTROMETER

5.1   Instrument Overview

Spectrometers show the spectrum of frequencies present in a signal. [12] Wave spec-
trometers allow for calculating the spectral power of higher frequency components associated
with plasma waves. There is a possible correlation between higher frequency components of
plasma density and the formation of plasma bubbles. The data obtained from the EFP and
SLP can be processed through a wave spectrometer to compute the spectral power. The
EFP and SLP spectrometer channels are used to observe higher frequency components in
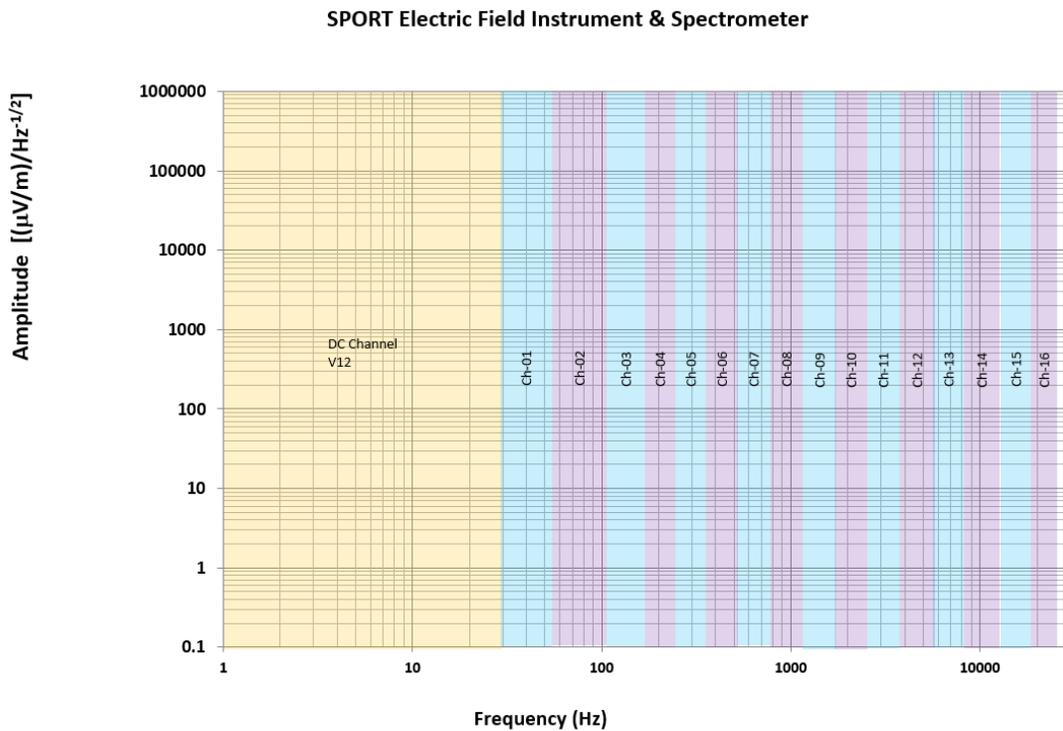16 power spectral bands.

Fig. 5.1: Wave Spectrometer Bins

Fig. 5.2: Location of Wave components on the USU SWP PCBA

5.1.1 Instrument Requirements

In order to meet the SPORT science requirements, it was determined that the Wave Spectrometer would need to be designed to meet the Functional requirements shown in Table 5.1. The test range used to verify each of these requirements is also shown. More detail on the testing is provided in the Calibration and Testing section at the end of this chapter.

Table 5.1: Key Wave Functional Requirements

Parameter	Units	Requirement	Test Range
EFP Wave Channels	Channels	16	16
SLP Wave Channels	Channels	16	16
Frequency Range	Hz	30 to 20,000	1 to 30,000

5.2 Design and Analysis

5.2.1 Analog Design

The wave channel EFP analog front end is connected to both EFP sensors. The two probes signals are differenced before passing through a high pass filter. The high pass filter was designed to have a cutoff frequency of 20 Hz. The output from the filter is converted to a differential signal to drive the ADC using the same driving circuit used previously for the EFP and SLP channels.
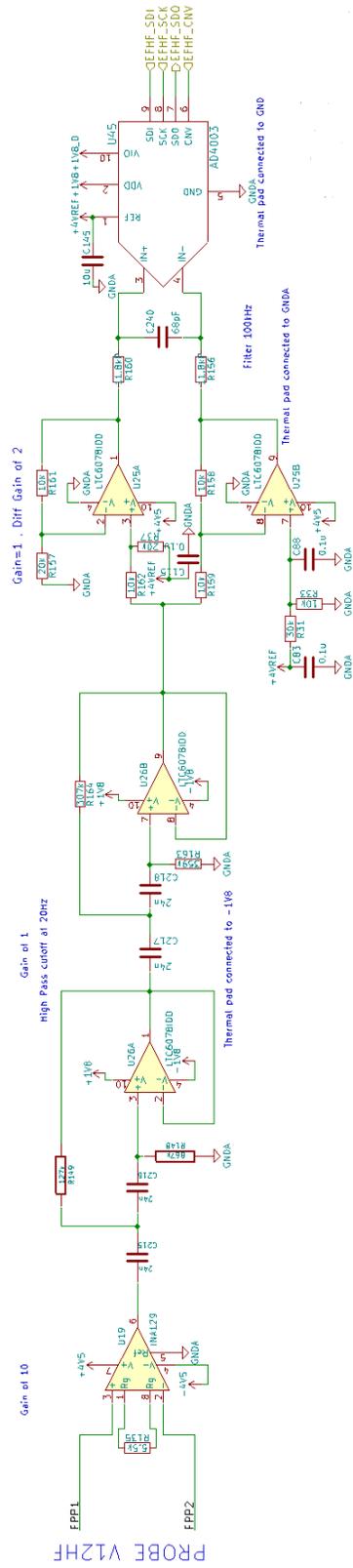
Fig. 5.3: Wave Channel

5.2.2   Digital Design

The EFP HF Wave channel ADC is sampled at 200 kHz. The SLG LG channel is sampled simultaneously. Both the EFP HF and SLP LG samples are averaged by 4 samples, reducing the sample rate to 50kHz. To reduce the resources in the FPGA both channels share the same FFT module. A mux is used to control which channel is running samples through the FFT. Each channel stores 1024 samples in RAM using the FFT Sample Store module until the FFT is available. When the FFT is ready to process a sample set, the 1024 samples are clocked in at 20 MHz, two samples per clock cycle. The FFT module after processing the sample set, clocks out the I and Q results at 20 MHz, two samples per clock cycle. At this point the mux is switched to allow the other channel's stored samples to be input to the FFT module. The I and Q results are then summed into 16 spectral bins in the FFT Bin sum module. Once all the bins have been summed, the output is sent to the Gather and Mask module. The Gather and Mask module reduces the FFT output words to 24 bits. The bits chosen are shown in the excel calculations in Figure 5.4. These calculations also show the FFT bins summed in each channel and the corresponding frequency ranges. The parameters for the wave give us the channel sensitivities shown in figure 5.5.

|	FFT Bins		TM Word		TM Word	Start	Mid	Stop	Width (B_w)
ID	Start	End	Start	Stop	bits.bins	0.0	25.0	50.0	50.0
Ch01	1	1	6	29	24.001	49	73.2	98	48.8
Ch02	2	2	5	28	24.001	98	122.1	146	48.8
Ch03	3	3	4	27	24.001	146	170.9	195	48.8
Ch04	4	5	4	27	24.002	195	244.1	293	97.7
Ch05	6	7	4	27	24.002	293	341.8	391	97.7
Ch06	8	10	4	27	24.003	391	463.9	537	146.5
Ch07	11	15	4	27	24.005	537	659.2	781	244.1
Ch08	16	23	4	27	24.008	781	976.6	1172	390.6
Ch09	24	33	4	27	24.010	1172	1416.0	1660	488.3
Ch10	34	49	3	26	24.016	1660	2050.8	2441	781.3
Ch11	50	73	3	26	24.024	2441	3027.3	3613	1171.9
Ch12	74	107	3	26	24.034	3613	4443.4	5273	1660.2
Ch13	108	159	3	26	24.052	5273	6543.0	7813	2539.1
Ch14	160	234	2	25	24.075	7813	9643.6	11475	3662.1
Ch15	235	346	2	25	24.112	11475	14209.0	16943	5468.8
Ch16	347	511	2	25	24.165	16943	20971.7	25000	8056.6

Fig. 5.4: Wave Telemetry Calculations
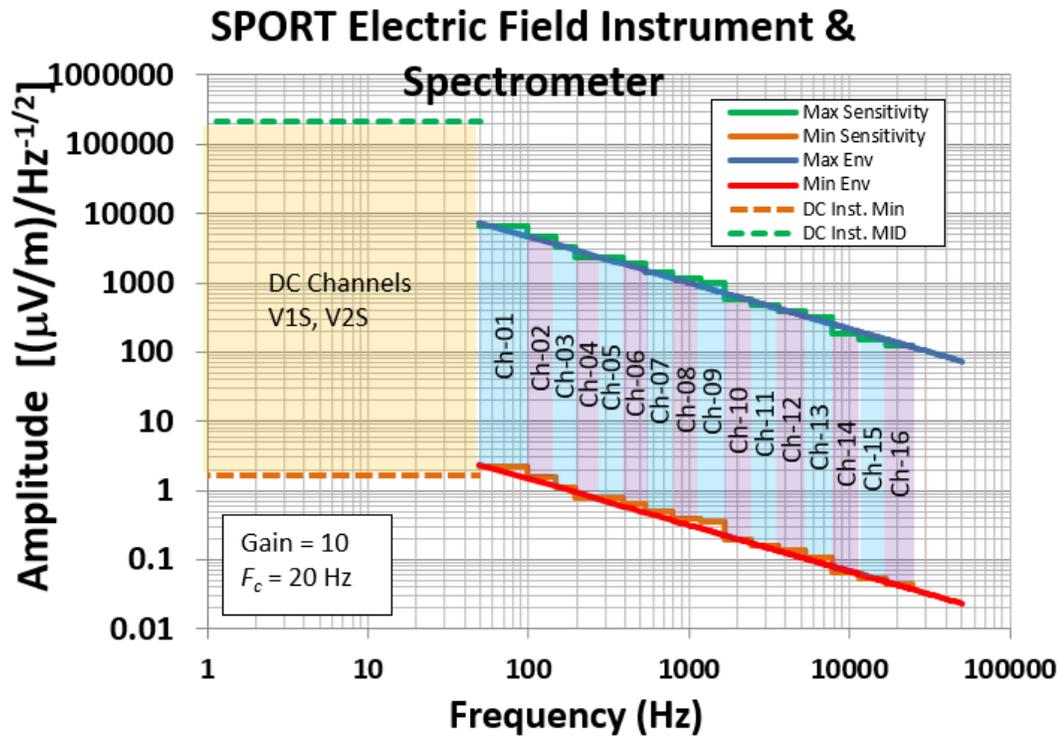
Fig. 5.5: Wave Channel Sensitivities (Boom $= 0.8m$)

The Gather and Mask module sums 4 granules each of both the EFP and SLP before averaging and sending the data to the APB FIFO. The EFP HF Wave channel ADC is the same ADC used in daisy chain mode for the SLP and EFP channels. For the wave channel, the ADC is used in normal operating mode.
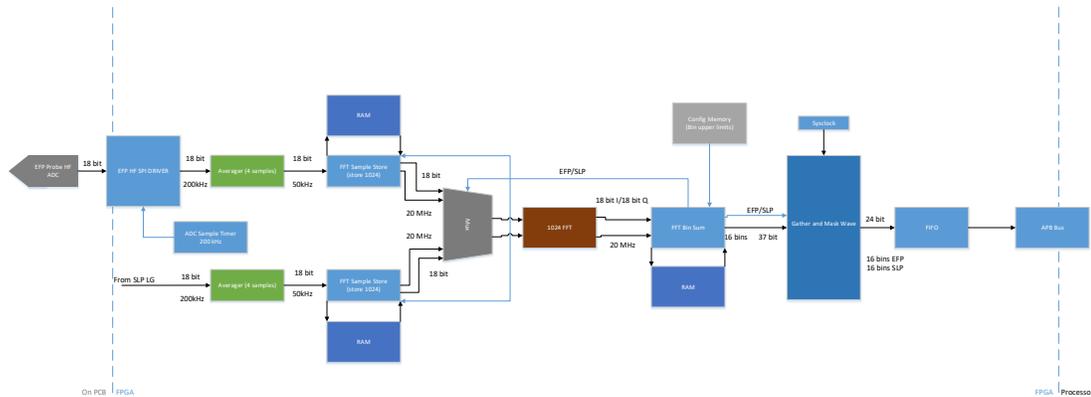

Fig. 5.6: FPGA flow diagram for Wave Spectrometer

5.3 Calibration and Testing

The Wave Spectrometer is tested and calibrated during the testing and calibration of the SLP and EFP.

5.3.1 Calibration Methodology

Wave Frequency Response

The purpose of this test is to determine the frequency response of each of the 16 electric field spectrometer channels. Sine waves are input into both the Electric Field Probes and the Sweeping Langmuir probe. The frequency was swept from 10 Hz to 100kHz in 100 log spaced steps per decade. The test was performed with EFP Sensors 1 and 3 to DC source and 2 and 4 grounded. Figure 5.7 shows a plot of EFP wave data from during a frequency sweep.
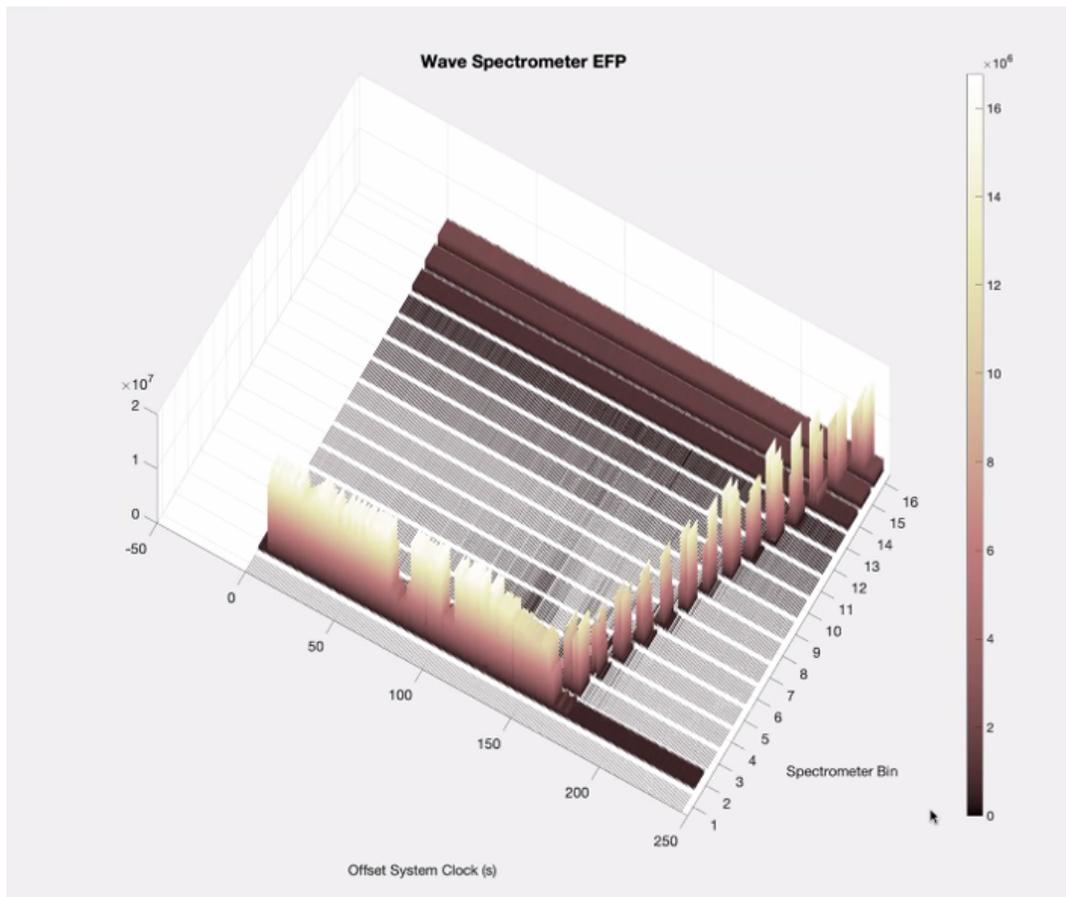
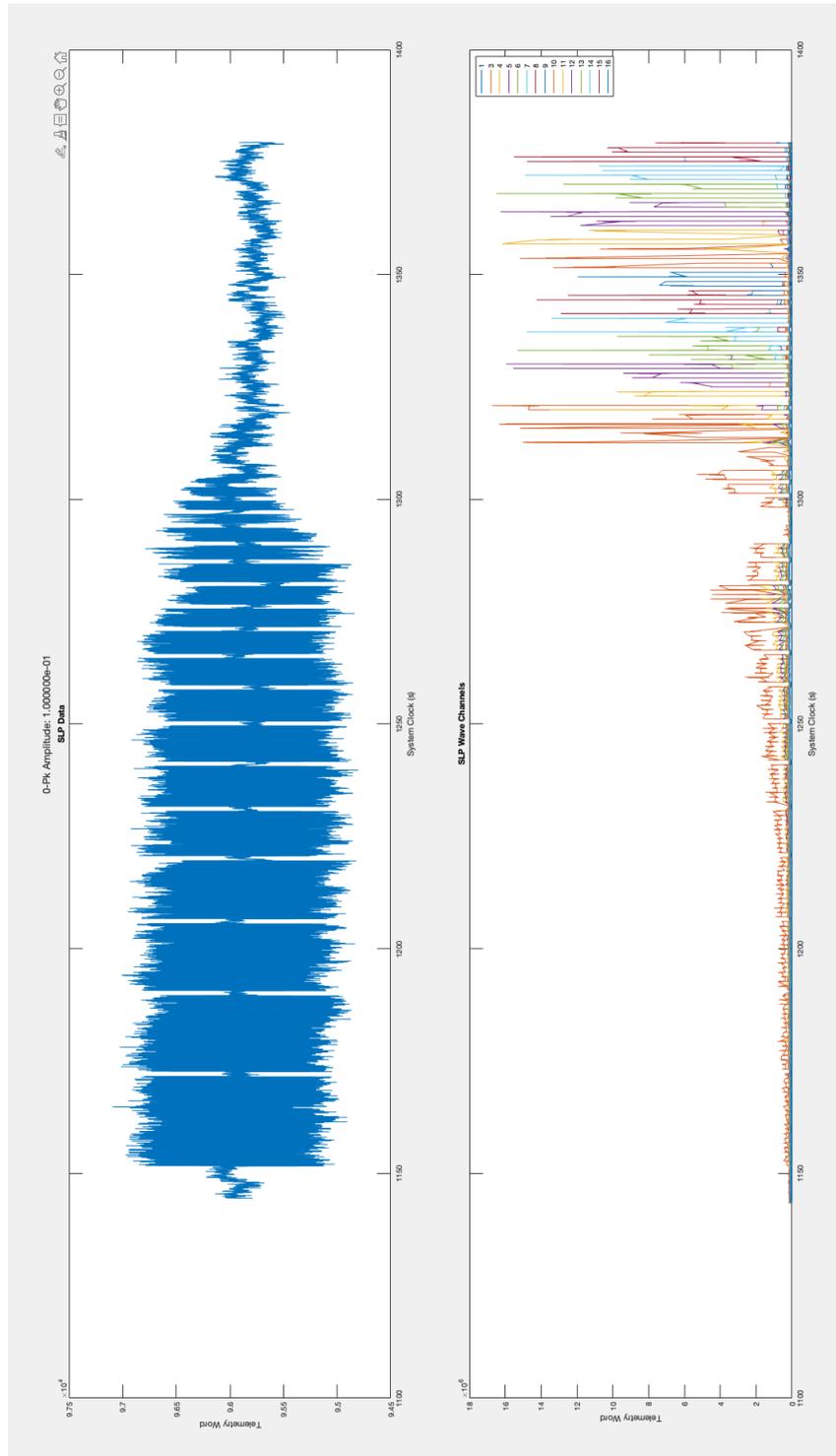Fig. 5.7: Wave Spectrometer results from EFP Frequency Sweep

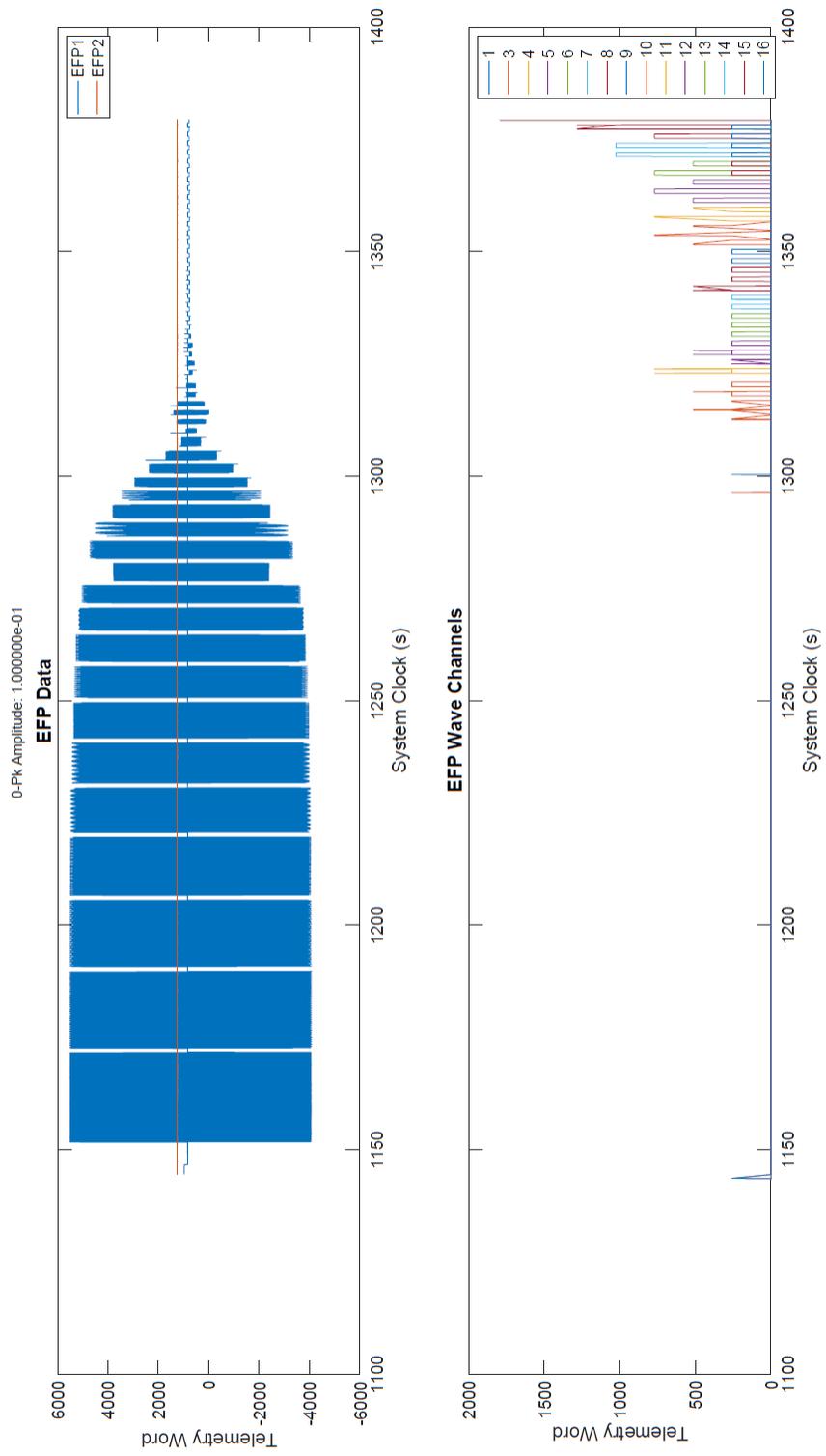Fig. 5.8: Wave Spectrometer results from SLP Frequency Sweep

Fig. 5.9: Wave Spectrometer results from SLP Frequency Sweep

CHAPTER 6

CONCLUSIONS

6.1 Performance Review

6.2 Lessons Learned and Future Work

6.2.1 Sweeping Langmuir Probe

The SLP has some non-linearity due to the analog front end of the instrument. The gain of the analog signal causes the signal to run into the common-mode input of the differential amplifier.

The SLP High gain channel had a potentiometer to trim the gain. However, this did not work properly and had to be removed from the PCBA. Adding the ability to trim the HG channel on a future revision would be a desired feature.

The power supply range of the SLP was too low. This caused many complications with the op-amp rails in the analog front end. The voltage range could be designed to be closer to $\pm 8v$ in a future revision.

The data rate of the SLP HG channel could be reduced. Averaging the output of the HG channel and only providing one measurement per Science packet would be sufficient.

6.2.2 Electric Field Probe

The INA116 has been used on multiple revisions of the Electric Field Probe. However, this IC is older and takes up a large amount of area on the PCBA. A future revision would change out the INA116 for a smaller, newer instrumentation amplifier IC.

6.2.3 Wave

Initially the Wave Spectrometer was going to implement a 2048-point FFT on both

the SLP and EFP channels, with each channel having its own FFT module. This design had to be modified due to the resource limitations of the Smartfusion 2 M2S025. The SoC model used did not have enough RAM block for the initial design. Upgrading to the next model, M2S050, would have provided the needed resources but would have added costs to the project due to software licensing fees and new hardware.

6.2.4 Overall System

The USU SWP Power conditioning system was revised several types during the design process to reduce power consumption. In an attempt to reduce power loss, the analog 5V was regulated down to 2.5V before being regulated again down to +- 1.8V. The 2.5V linear voltage regulator did not work as expected and would become damaged on power up. Removing this IC was required for the board to operate but increased the power loss from the 5 to 1.8 V regulation. The Smartfusion 2 SoC was used on an Emcraft SOM daughter board. The daughter board connected to the main PCBA using two 80 pin connectors. During development we had several issues with these connectors, causing setbacks to the project timeline. In a future revision of the SWP, the FPGA would most likely be placed directly on the main PCBA. The current SOM daughter board did decrease complexity and speed up the initial development of the SWP. However, there are several components on the SOM that were either not utilized in this project or were not conducive towards the power consumption requirements. A specific example of this is the onboard LPDDR memory, which we had problems developing with and is a suspect of large power consumption. A future revision without this SOM would be able to eliminate unnecessary components and change higher power components to further reduce overall system power consumption. Headers for ethernet and debugging buttons were added to the PCB. However, these were never used during development. An increased number of LEDs and test points would have been more useful for debugging. There are some specific points in the circuit where it would have been convenient to have a test point. During initial bring up of the SWP hardware it was difficult to determine what ICs were causing high current draw. On the engineering model of the SWP, it would have been convenient to have more jumpers/0-ohm resistors

to disconnect the voltage supply to ICs during debugging. The RTC resets on power loss to a default reset value. This reset value cannot be changed. A different RTC without this behavior should be selected for a future revision. A more sensitive magnetometer would be selected in a future revision.

REFERENCES

[1] L. H. Brace, "Langmuir probe measurements in the ionosphere," in *Measurement Techniques in Space Plasmas*, ser. Particles, D. T. Y. Robert F. Pfaff, Joseph E. Borovsky, Ed. American Geophysics Union, 1998, pp. 23–35.

[2] S. R. Burr, "The design and implementation of the dynamic ionosphere cubesat experiment (dice) science instruments," Master's thesis, Utah State University, Logan, UT, 2013.

[3] C. Fish, C. Swenson, T. Neilsen, B. Bingham., J. Gunther, E. Stromber, S. Burr, R. Burt, M. Whitely, G. Crowley, I. Azeem, M. Pilinski, A. Barjatya, and J. Petersen, "Dice mission design, development, and implementation: Success and challenges," in *Proc. AIAA/Utah State University Conference on Small Satellites*, 2012.

[4] C. S. Fish, C. M. Swenson, G. Cowley, A. Barjatya, T. Neilsen, J. H. Gunther, R. R. Fullmer, R. Baktur, and J. J. Sojka, "Design, development, implementation, and on-orbit performance of the dynamic ionosphere cubesat experiment mission," in *Space Science Reviews*, 2014.

[5] D. Farr, "Resolving the temporal-spatial ambiguity with the auroral spatial structures probe," Master's thesis, Utah State University, Logan, UT, 2014.

[6] J. D. Gregory, "Design, test, and calibration of the utah state university floating potential probe," Master's thesis, Utah State University, Logan, UT, 2010.

[7] F. L. Scarf and D. A. Gurnett, "A plasma wave investigation for the voyager mission," in *Space Science Reviews*, ser. 21. Kluwer Academic Publishers, 1977, pp. 289–308.

[8] D. Young, J. Berthelier, M. Blanc, J. Burch, A. Coates, R. Goldstein, M. Grande, T. Hill, R. Johnson, V. Kelha, D. Mccomas, E. Sittler, K. Svenes, K. Szegö, P. Tanskanen, K. Ahola, D. Anderson, S. Bakshi, R. Baragiola, B. Barraclough, R. Black, S. Bolton, T. Booker, R. Bowman, P. Casey, F. Crary, D. Delapp, G. Dirks, N. Eaker, H. Funsten, J. Furman, J. Gosling, H. Hannula, C. Holmlund, H. Huomo, J. Illiano, P. Jensen, M. Johnson, D. Linder, T. Luntama, S. Maurice, K. Mccabe, K. Mursula, B. Narheim, J. Nordholt, A. Preece, J. Rudzki, A. Ruitberg, K. Smith, S. Szalai, M. Thomsen, K. Viherkanto, J. Vilppola, T. Vollmer, T. Wahl, M. Wüest, T. Ylikorpi, and C. Zinsmeyer, "Cassini plasma spectrometer investigation," in *Space Science Reviews*, 1977, pp. 1–112.

[9] J. Bourgeret, M. Kaiser, P.J.Kellogg, R. Manning, K.Goetz, S.J.Monson, N.Monge, L. Friel, C. Meetre, C. Perche, L. Sitruk, , and S. Hoang, "Waves: the radio and plasma wave investigation on the wind spacecraft," in *Space Science Reviews*. Kluwer Academic Publishers, 1995, pp. 231–263.

[10] A. Barjatya, "Langmuir probe measurements in the ionosphere," Ph.D. dissertation, Utah State University, Logan, UT, 2007.

[11] A. Pedersen, F. Mozer, and G. Gustafsson, "Electric field measurements in a tenuous plasma with spherical double probes," in *Measurement Techniques in Space Plasmas*, ser. Fields, D. T. Y. Robert F. Pfaff, Joseph E. Borovsky, Ed. American Geophysics Union, 1998, pp. 1–12.

[12] D. A. Gurnett, "Principles of space plasma wave instrument design," in *Measurement Techniques in Space Plasmas*, ser. Fields, D. T. Y. Robert F. Pfaff, Joseph E. Borovsky, Ed. American Geophysics Union, 1998, pp. 121–137.
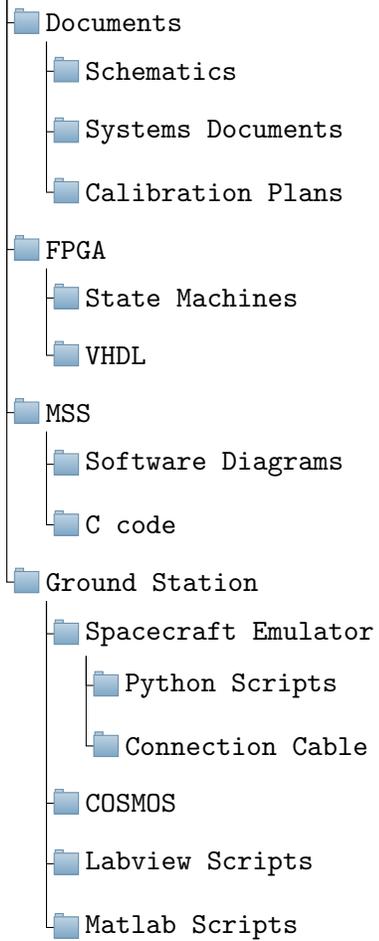
APPENDICES

APPENDIX A

DVD Contents

The DVD included with this thesis includes all files and documents related to the USU

SPORT SWP

```
USU SPORT SWP
├── Documents
│   ├── Schematics
│   ├── Systems Documents
│   └── Calibration Plans
├── FPGA
│   ├── State Machines
│   └── VHDL
├── MSS
│   ├── Software Diagrams
│   └── C code
└── Ground Station
    ├── Spacecraft Emulator
    │   ├── Python Scripts
    │   └── Connection Cable
    ├── COSMOS
    ├── Labview Scripts
    └── Matlab Scripts
```
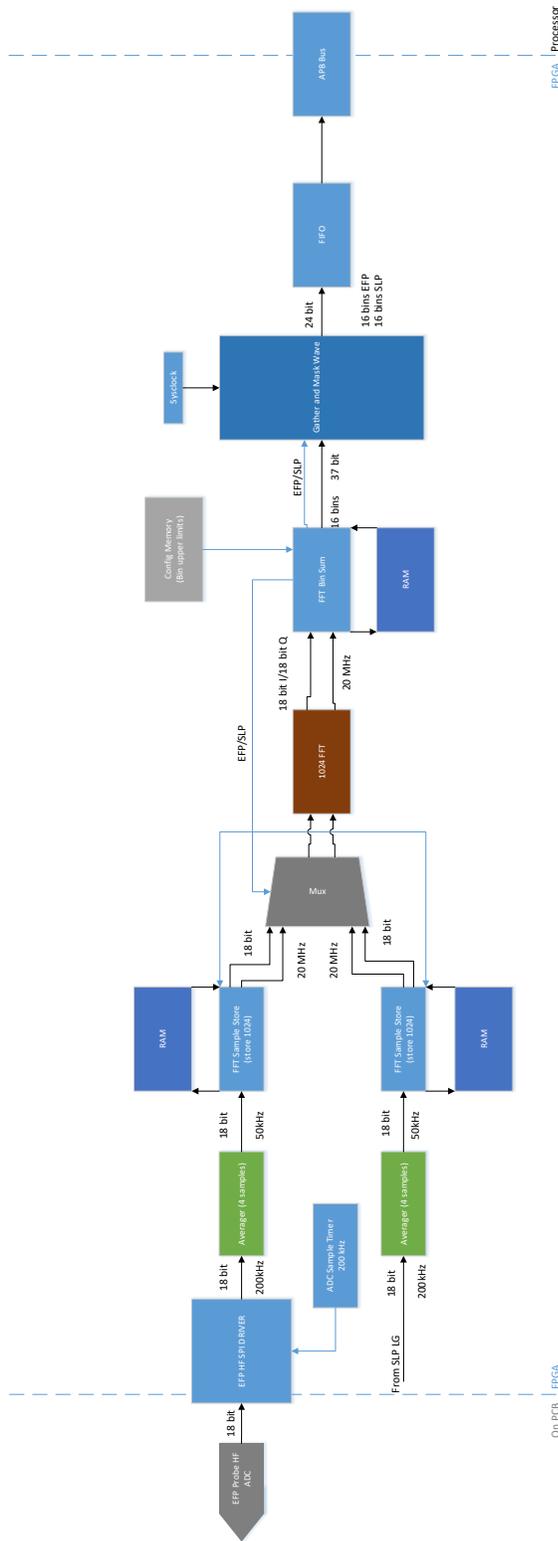
APPENDIX B

Flow Diagrams

Fig. B.1: FPGA Flow Diagram for Wave Enlarged